Original Article

MOLECULAR METABOLISM

Reduced liver mitochondrial energy metabolism impairs food intake regulation following gastric preloads and fasting

Michael E. Ponte[1,8], John C. Prom[1,8], Mallory A. Newcomb[1], Annabelle B. Jordan[1], Lucas L. Comfort[1], Jiayin Hu[4], Patrycja Puchalska[5], Devin C. Koestler[6], Caroline E. Geisler[4,7], Matthew R. Hayes[4], E. Matthew Morris[1,2,3,*]

ABSTRACT

Objective: The capacity of the liver to serve as a peripheral sensor in the regulation of food intake has been debated for over half a century. The anatomical position and physiological roles of the liver suggest it is a prime candidate to serve as an interoceptive sensor of peripheral tissue and systemic energy state. Importantly, maintenance of liver ATP levels and within-meal food intake inhibition is impaired in human subjects with obesity and obese pre-clinical models. Previously, we have shown decreased hepatic mitochondrial energy metabolism (i.e., oxidative metabolism & ADP-dependent respiration) in male liver-specific, heterozygous PGC1a mice results in increased short-term diet-induced weight gain with increased within meal food intake. Herein, we tested the hypothesis that decreased liver mitochondrial energy metabolism impairs meal termination following nutrient oral pre-loads.

Methods: Liver mitochondrial respiratory response to changes in ΔG_{ATP} and adenine nucleotide concentration following fasting were examined in male liver-specific, heterozygous PGC1a mice. Further, food intake and feeding behavior during basal conditions, following nutrient oral pre-loads, and following fasting were investigated.

Results: We observed male liver-specific, heterozygous PGC1a mice have reduced mitochondrial response to changes in ΔG_{ATP} and tissue ATP following fasting. These impairments in liver energy state are associated with larger and longer meals during chow feeding, impaired dose-dependent food intake inhibition in response to mixed and individual nutrient oral pre-loads, and greater acute fasting-induced food intake.

Conclusions: These data support previous work proposing liver-mediated food intake regulation through modulation of peripheral satiation signals.

Keywords Liver; Mitochondria; ATP; Food intake; Satiation; Fasting

1. INTRODUCTION

The increased food intake associated with weight gain occurs through an imbalance of external obesogenic food cues and interoceptive satiation signals [1—4]. Predisposition to weight gain can result from a hypersensitivity to hunger interoceptive signals and/or insensitivity to satiety interoceptive signals [5]. Gastrointestinal (GI)-derived interoceptive satiation signals in the form of mechanoreception, neuropeptides, and neurotransmitters communicate nutrient-state dependent information primarily through vagal afferent neurons to the brain to regulate feeding behavior (reviewed [6—10]). These signals relay the size and nutritive composition of the material in the GI tract in a temporospatial manner, culminating in meal termination [11—17]. Reductions in the magnitude of these satiation signals delays meal termination, resulting in larger within-meal food intake and overall greater energy intake, leading over time to subsequent weight gain [18]. Importantly, human subjects with overweight/obesity and diet-induced obese pre-clinical rodent models have decreased satiation signaling following overfeeding [19], reduced vagal afferent expression of satiation signal receptors [20], reduced secretion and/or response to GI-derived satiation signals [21—30], decreased satiation in response to gastric and intestinal nutrients [31], and reduced vagal afferent excitability in response to nutrients [32]. Collectively, these maladaptive phenotypes contribute to the reduction of within-meal food intake inhibition. While visceral vagal afferents are sensitive to GI factors to induce meal termination, absorbed nutrients and hormones generate

[1]Depatment of Cell Biology & Physiology, University of Kansas Medical Center, Kansas City, KS, USA [2]Center for Children's Healthy Lifestyle and Nutrition, Children's Mercy Hospital, Kansas City, MO, USA [3]University of Kansas Diabetes Institute, Kansas City, KS, USA [4]Department of Psychiatry, University of Pennsylvania, Philadelphia, PA, USA [5]Division of Molecular Medicine, University of Minnesota, Minneapolis, MN, USA [6]Department of Biostatistics, University of Kansas Medical Center, Kansas City, KS, USA [7]Department of Pharmaceutical Sciences, University of Kentucky, Lexington, KY, USA

[8] These authors contributed equally to this work.

*Corresponding author. Department of Molecular and Integrative Physiology, 3901 Rainbow Boulevard, Hemenway Life Sciences Innovation Center, Mailstop 3043, University of Kansas Medical Center, Kansas City, KS, 66160, USA. E-mail: emorris2@kumc.edu (E.M. Morris).

Received April 10, 2025 • Revision received May 6, 2025 • Accepted May 7, 2025 • Available online 12 May 2025

https://doi.org/10.1016/j.molmet.2025.102167

signals originating from hepatic portal vein and liver parenchyma to activate hepatic vagal afferents in the regulation of food intake.

Due to the liver's numerous catabolic/anabolic metabolic processes and location in the splanchnic circulation, considerable changes in energy demand occur during transitions from prandial to postprandial states [33]. However, hepatocytes cannot store high energy phosphate as phospho-creatine like skeletal muscle [34,35]. Thus, during high energy demand the liver can only maintain ATP levels (ATP homeostasis) by increasing mitochondrial energy metabolism ([MEM], i.e., oxidative metabolism, ADP-dependent respiration). As such, the liver is anatomically and physiologically well placed to serve as an interoceptive sensor of peripheral tissue and systemic energy state. To this end, the liver was first proposed to regulate food intake through glucose sensing [36]. Numerous subsequent publications demonstrated increased food intake in association with vagal transmission [37–40] of chemically reduced hepatic fatty acid oxidation [41–49] and/or depleted hepatic ATP levels in rodents [50–53]. Importantly, oral delivery of the fatty acid oxidation inhibitor etomoxir to human subjects stimulated acute food intake [54]. However, the high potential for off-site action of intraperitoneal delivered chemical inhibitors and use of vagotomy reduced the rigor of these findings. The use of direct genetic manipulations of hepatic energy state on appetite control is necessary to elucidate the presence of a liver interoceptive sensing mechanism.

Previously, we have reported increased short-term diet-induced weight gain and greater high-fat diet food intake in rats with reduced hepatic MEM [55–57]. However, the hepatic mitochondrial phenotype is present as part of the models differences in intrinsic aerobic fitness based on selective breeding [58], complicating determination of any mechanism(s) responsible for the differences in energy homeostasis. More recently, we observed increased short-term diet-induced weight gain, high-fat diet food intake, and within-meal consumption in a mouse model of reduced liver MEM due to liver-specific reductions in the expression of the mitochondrial co-transcriptional regulator, PGC1a (LPGC1a+/−) [59]. While we have previously observed liver-specific overexpression of PGC1a increases hepatic MEM, it is still unclear whether reduced liver MEM in LPGC1a+/− mice negatively impacted tissue ATP homeostasis and meal termination.

Combining these data with the previous pharmacological findings, we hypothesize that inhibition of food intake via nutrient-induced, GI-derived satiation signals is decreased under conditions of impaired hepatic ATP homeostasis. To test this hypothesis, we again used the liver-specific, PGC1a heterozygous mouse model. We and others have shown that LPGC1a+/− mice have reduced expression of β-oxidation genes, impaired mitochondrial complete fatty acid oxidation, and diminished maximal mitochondrial respiratory capacity [59,60]. Herein, we assessed whether the LPGC1a+/− mouse has impaired food intake inhibition in response various nutritional challenges to finally establish a direct link between hepatic MEM and satiation.

2. METHODS

2.1. Ethical approval

The animal protocol was approved by the Institutional Animal Care and Use Committee at the University of Kansas Medical Center. All experiments were carried out in accordance with the *Guide for the Care and Use of Laboratory Animals* published by the US National Institutes of Health (NIH guide, 8th edn, 2011). Male liver-specific PGC1a heterozygous (LP) mice were produced as previously described [59,60]. Briefly, male C57Bl6/J mice (#000664, Jackson Laboratory, Bar Harbor, ME, USA) were mated with female PGC1a homozygous floxed mice (#009666, Jackson Laboratory, Bar Harbor, ME, USA) to generate heterozygous PGC1a flox mice. Female PGC1a fl/+ mice were bred to albumin-cre recombinase mice (#003574, Jackson Laboratory, Bar Harbor, ME, USA) to generate liver-specific PGC1a heterozygous and wildtype (WT) littermates. Mice were housed at 28 °C on 12/12 reverse light cycle (dark 10:00—20:00), with *ad lib* access to water and normal chow.

2.2. Genotyping

Mouse and liver-specific genotypes were confirmed as previously described [60]. The primers used are listed below.

2.3. Food intake regulation

LP and WT mice were acclimated to individual housing and oral gavage in BioDAQ cages (Research Diets Inc., New Brunswick, NJ) for 3 weeks prior to the initiation of the food intake regulation studies. On experimental days (Monday & Thursday), mice were food restricted at 0800, underwent gavage at 0930, and food access and data collection began at 1000. Sham gavage experiments were performed periodically to assess basal feeding throughout the study (n=4 sham). Additional, basal food intake data was collected during the non-experimental days (n = 9). Basal food intake data presented represents the combined average of each mouse across all sham treatments and non-experimental days collected (Figure 2A). Ensure powder (Abbot Nutritional Products, Abbott Park, IL) was resuspended in MilliQ water to produce a 5 kcal/mL solution, and dosed at 5, 10, and 15 mL/kg. This resulted in the delivery of ∼1.5 kcal at the 10 mL/kg dose (30 g mouse), which represents about ∼15% of the kcals consumed in 24hr or the approximate energy intake during the first 2 h of the dark cycle. Methylcellulose (M0512, Sigma Aldrich, St. Louis, MO) was dissolved in normal saline at 1% & 2% by weight and delivered at 10 mL/kg. Antagonists of peripheral satiation receptors 5-HT3R (ondansetron, 5 mg/kg, saline, PHR1141, Sigma Aldrich, St. Louis, MO), CCK-1R (lorglumide, 0.3 mg/kg, saline, 17555, Caymen Chemicals, Ann Arbor, MI), and GLP1R (exendin-9, 100 μg/kg, saline, 4017799, Bachem, Torrance, CA) were delivered IP, 30 min before the initiation of oral gavage of 10 mL/kg Ensure. Intralipid (Baxter, Deerfield, IL), 40% glucose (D16, Thermo Fisher Scientific, Waltham, MA), and Proteinex (Llorens Pharmaceutical, Miami, FL) were delivered via oral gavage at 10 and 15 mL/kg to assess specific macronutrient oral pre-load inhibition of food intake. This results in the delivery of 0.6 kcal of lipid and protein, and 0.48 kcal of glucose at the 10 mL/kg dose. For fasting-induced acute food intake experiments, the BioDAQ gates were closed at 1600 resulting in an 18hr fast, with food intake measurements beginning at 1000. BioDAQ data analysis was binned at 0.5 h or 1 h intervals using BioDAQ Data Viewer (ver. 2.3.14, BioDAQ, Research Diets Inc. New Brunswick, NJ), with inter-meal interval and minimum meal mass set at 90 s and 0.05 g, respectively.

2.4. Plasma GI-derived satiation signal concentration

Following a 2 h food restriction mice received a 5 mL/kg oral gavage of Ensure, as described above. Blood was collected 90 min following the

Primer table

Genotyping		Forward Primer	Reverse Primer
Tail	**LoxP sites**	TCC AGT AGG CAG AGA TTT ATG AC	TGT CTG GTT TGA CAA TCT GCT AGG TC
	Alb-cre	TTA GAG GGG AAC AGC TCC AGA TGG	GTG AAA CAG CAT TGC TGT CAC TT
Liver	**WT PGC1a**	CCA GTT TCT TCA TTG GTG TG	ACC TGT CTT TGC CTA TGA TTC
	Mutant PGC1a	TCC AGT AGG CAG AGA TTT ATG AC	CCA ACT GTC TAT AAT TCC AGT TC

oral nutrient gavage in anesthetized mice. Blood was added to EGTA coated tubes, plasma was collected following centrifugation (4 °C, 8,000×*g*, 10 min), and stored at −80 °C. Plasma 5-HT (LS-F40041, LS Bio, Shirley, MA), CCK (EIAM-CCK, RayBiotech, Norcross, GA), and GLP-1 (LS-F23033, LS Bio, Shirley, MA) concentration was determined as described by the manufacturer.

2.5. Liver mitochondria isolation

Liver mitochondria were isolated as previously described [59]. Briefly, following a 2-hr food withdrawal (0800−1000), ∼1 g of liver was collected from anesthetized mice and homogenized (glass-on-teflon) in 8 mL of ice-cold mitochondrial isolation buffer (220 mM mannitol, 70 mM sucrose, 10 mM Tris, 1 mM EDTA, pH adjusted to 7.4 with KOH). The homogenate was centrifuged (4 °C, 10 min, 1500 g), the supernatant was transferred to a round bottom tube, and centrifuged (4 °C, 10 min, 8000×*g*). The pellet was resuspended in 6 mL of ice-cold mitochondrial isolation buffer using a glass-on-glass homogenizer, and centrifuged again (4 °C, 10 min, 6000×*g*). The pellet was resuspended in 4 mL of isolation buffer containing 0.1% BSA and centrifuged (4 °C, 10 min, 4000×*g*). This final pellet was resuspended in ∼0.75 mL of mitochondrial respiration buffer (0.5 mM EGTA, 3 mM MgCl2, 60 mM KMES, 20 mM glucose, 10 mM KH2PO4, 20 mM HEPES, 110 mM sucrose, 0.1% BSA, 0.0625 mM free CoA, and 2.5 mM carnitine, pH∼7.4). The protein concentration of the final suspension was determined by BCA assay.

2.6. Liver mitochondrial creatine kinase clamp

Creatine kinase clamp technique was used in isolated liver mitochondria to assess respiration under physiologically relevant energy demand, and the capacity of mitochondria to increase respiration in response to changes in ATP free energy states (ΔG_{ATP}) [61,62]. Briefly, 2 mM malate, isolated liver mitochondria, 10 μM palmitoyl-CoA, 10 μM palmitoyl-carnitine, 5 mM ATP, 5 mM creatine, and 20 U/mL creatine kinase were added to Oroboros chambers containing mitochondrial respiration buffer. ADP-dependent respiration was initiated by the addition of 1 mM PCr, and sequential additions of PCr to 3, 6, 9, 12, 15, 18, 21, 24, 27, 30 mM reduced respiration toward baseline. Oxygen consumption values were normalized to total protein within the chamber. The free energy of ATP for each PCr concentration was calculated as described [61]. The capacity to increase mitochondrial respiration in response to changes in ΔG_{ATP} (conductance) was calculated as the slope of the linear respiration data from 9 mM to 21 mM PCr. The data is oriented to represent an simulated increase in energy demand produced by the clamp.

2.7. Fasting/re-feeding

Mice had food withdrawn for 2hrs or overnight (18hrs, 1600−1000). This fasting paradigm represents a more physiologically relevant regimen as the food was removed halfway through the dark cycle, from fed mice. Re-feed mice were allowed access to normal chow for 4 h following the fast. Mice were anesthetized with 100 mg/kg phenobarbital, and a section of the liver was clamp frozen. The brain was frozen in 2-methyl-butane and both tissues were stored at −80 °C.

2.8. Liver adenine nucleotide pool

Measurement of liver adenine nucleotide pool was performed by the University of Minnesota Metabolomics Core. Clamp frozen liver sections were weighed and homogenized using zirconium beads in 0.4 M perchloric acid, 0.5 mM EGTA extraction solution containing [$^{13}C_{10}$, $^{15}N_5$]ATP sodium salt (100 mM), [$^{13}C_{10}$, $^{15}N_5$]AMP sodium salt (100 mM), [1,2−$^{13}C_2$]acetyl-CoA lithium salt (5 mM), and [1,2,3−$^{13}C_3$] malonyl-CoA lithium salt (5 mM). After incubation on ice for 10 min, samples were centrifuged at 15,000×*g* for 15 min at 4 °C. The resulting supernatants were neutralized with freshly prepared 0.5 M K_2CO_3, vortexed, and centrifuged at 15,000×*g* for 30 min at 4 °C. Final extracts were then analyzed by LC-MS/MS as previously described [63,64], with modifications. Energy charge was calculated as (ATP + (0.5 × ADP))/(ATP + ADP + AMP).

2.9. Liver & hypothalamus RNA expression

Liver RNA was isolated from ∼25 mg of liver tissue using an RNeasy Plus Mini Kit (Qiagen, Valencia, CA, USA) and hypothalamus RNA was isolated using the standard Triazol procedure. The cDNA for both tissues was produced using the ImProm-II RT system (Promega, Madison, WI, USA). RT-PCR was performed using a Bio-Rad CFX Connect Real-Time System (Bio-Rad, Hercules, CA, USA) and SYBR Green. The SYBR green primers are listed below. Gene specific values for liver were normalized to relative cyclophilin B (*ppib*) mRNA expression values and hypothalamus gene specific values were normalized to Tryptophan 5-Monooxygenase Activation Protein Zeta (*ywhaz*) mRNA expression values.

2.10. Liver glycogen concentration

Liver glycogen was determined as previously described [65]. Briefly, ∼15−30 mg of liver was solubilized in 0.5 mL of 1 N HCl in boiling water for 1.5−2.0 h. Samples were neutralized by adding 1.5 mL of

RT-PCR	Forward Primer	Reverse Primer
PGC1a (exon 3−5)	AGC CGT GAC CAC TGA CAA CGA G	GCT GCA TGG TTC TGA GTG CTA AG
PEPCK	AATATGACAACTGTTGGCTG	AATGCTTTCTCAAAGTCCTC
HADHA	ATAATTGATGCTGTGAAGGC	TCTCCAAATTTCTGCGATTC
PGC1b	AAGAACTTCAGACGTGAGAG	TCAAAGCGCTTCTTTAGTTC
PPRC1	AAACTCAGGCATTGACATTC	CGGTGGATTTAGGAGATTTG
NT-PGC1a	TGCCATTGTTAAGACCGAG	GGTCACTGGAAGATATGG
UCP2	ACCTTTAGAGAAGCTTGACC	TTCTGATTTCCTGCTACCTC
NRF1	AAACAAAGGGTTTCATGGAC	GGTACGAGATGAGCTATACTG
TFAM	GACCTCGTTCAGCATATAAC	ACAAGCTTCAATTTTCCCTG
GAPBA	GAGATAGTTACCATTGACCAG	GACCATTGTTTCCTGTTCTG
COX4I2	TCTATGTGTTCCCTAAGAAGG	CCACTCCTTCTTTTCATAATCCC
HMGCS2	AGAGCAATTTTACCACAAGG	TTTAAGCAGATGCTGTTTGG
PPARalpha	GATGTCACACAATGCAATTC	CAGTTTCCGAATCTTTCAGG
PPARdelta	CTGACAGATGAAGACAAACC	CTTCCTCTTTCTCCTCTTCC
PPARgamma	AAAGACAACGGACAAATCAC	GGGATATTTTTGGCATACTCTG
CPT1a	CTCCGCCTGAGCCATGAAG	CACCAGTGATGATGCCATTCT
ACOX1	GGATGGTAGTCCGGAGAACA	AGTCTGGATCGTTCAGAATCAAG
HNF4alpha	TCCTAGGCAATGACTACATC	CTGGATCAAAGAAGATGATGG
FOXO1	GCAGCCAGGCATTCATAA	CCTACCATAGCCATTGCAGC
ATP1A1	ACATGTGGTTTGACAATCAG	TACTGCCCGCTTAAGAATAG
ATP1B1	GGCAAGAGAGATGAAGATAAG	GTAGGGATAATACTGCAGAGG
ATP1B3	CCAGGACTTATGGTTTTTCC	CTATAGTCAGGACCATGCTG
FXYD1	CATTCACCTACGATTACCAC	CTCTTGCTAAGGATGATAAGG
FXYD5	ATCCAAAAACTTCATGCCTC	GTAGTATCATCGTAGTAGAAGGG
FXYD6	TTTCTATTACGACTACCAGACC	CGTTTGTAGTGATGAGGTTC
ATP2B1	CTTCTGGGTTCAGAAAAGAC	TTTTCTTGACTGAGTAAGCC
ATP2B2	ACATGCACAAGAAAGAGAAG	TGTAAGTAGAGTACCAGGATG
ATP2B4	CATTTGGTCCGATAAGACAG	TTCTGGAGGCTGAATCTTAG
FGF21	CAGTCCAGAAAGTCTCCTG	AGAAACCTAGAGGCTTTGAC
GDF15	AGCCGAGAGGACTCGAACTCA	TGGGACCCCAATCTCACCTCT
LEAP2	AGACTATGCAGAAAAAGACC	TATCTCCAACCAAAATGTCC
Angptl4	ATGGAGTAGACAAGACTTCG	TCACAGTTGACCAAAAATGG
FetuA	ACACACAGAATAATGGAACC	CTATTACAAACTCCACCAGAG
FetuB	AGAAAGACTCATACAACGTG	TATTCCACATAGTAAGCAGGG
AgRP	AGGTCTAAGTCTGAATGGC	CGGTTCTGTGGATCTAGC
POMC	AAAAGAGGTTAAGAGCAGTG	ACATCTATGGAGGTCTGAAG
NPY	AATCTCATCACCAGACAGAG	CTTTCCTTCATTAAGAGGTCTG

0.67 M NaOH. Free glycosyl units were determined spectrophotometrically using a glucose oxidase kit.

2.11. Liver mitochondrial content

While techniques to assess skeletal muscle mitochondrial content are validated [66], the appropriate assessment in liver is still debated. Herein, Cox4i2 mRNA expression was used as it's expression positively correlates with mtDNA concentration [67], and citrate synthase activity has previously been published as a marker [68–70]. Briefly, frozen liver was homogenized in 0.175 mM KCl, 2.0 mM EDTA (pH = 7.4) and centrifuged at 2,000×*g* (4 °C) for 5 min. Supernatants were freeze/thawed three times prior to initiation of assay. Aliquots of tissue homogenate were diluted in reaction buffer (100 mM Tris, 1.0 mM DTNB, 10 mM oxaloacetate, pH∼8.3). The reaction was initiated by the addition of 3 mM acetyl-CoA, and kinetic reads were taken at 412 nm every minute for 7 min (37 °C). Values were normalized to BCA of the homogenate.

2.12. Fluorescent *in situ* hybridization

Four-hour fasted wildtype and LPGC1a+/− mice were transcardially perfused with 0.1 M PBS followed by 4% paraformaldehyde in 0.1 M PBS on ice. Brains were removed, post-fixed in 4% paraformaldehyde for 24h, then stored in 20% sucrose in 0.1 M PBS at 4 °C until sunk. Coronal hypothalamic sections (20 μm) were sliced on a cryostat, dry mounted onto slides, and stored at −80 °C for future fluorescent *in situ* hybridization (FISH) processing. FISH to quantify mRNA expression of AgRP and POMC neuropeptides was performed using the RNAscope Multiplex Fluorescent V2 kit (323110, Advanced Cell Diagnostics, Inc.) according to manufacturer's instructions. The probes used were: mmPOMC (314081, Advanced Cell Diagnostics, Inc.) and mmAgRP (400711-C2, Advanced Cell Diagnostics, Inc.). Upon completion of the FISH protocol, slides were then coverslipped with Fluoromount G (0100-01, SouthernBiotech). Slides were visualized using fluorescence microscopy (BZ-X810, Keyence) and image analysis to quantify fluorescent signal of POMC and AgRP at weak, moderate, and strong intensity levels was performed using the HALO® Area Quantification FL module and expressed as total fluorescent area (μm^2).

2.13. Statistical analysis

Data are presented as means and standard error. The two-standard deviation test was utilized to test for outliers within group. Food intake, mitochondrial respiration, and *in situ* hybridization data (Figures 1A, 2-6, 7D & E) were assessed using the two-sample t-test between genotypes within level (e.g., ATP free energy state or time point). Inclusion of lines connecting time points in food intake data was for qualitative depiction only. Fasting/re-feeding (Figure 1B—N) and hypothalamus mRNA expression (Figure 7A—C) data were assessed by two-way ANOVA. When significant main effects and/or interactions for the independent variables were observed, scientifically relevant uncorrected pairwise comparisons were performed using Fisher's LSD. Main effects are only designated when all pairwise comparisons within the independent variable were significant.

3. RESULTS

3.1. Male LPGC1a+/− mice have decreased liver mitochondrial respiration in response to increasing energy demand and impaired ATP Homeostasis During Fasting

The liver has been proposed to regulate food intake through interoceptive vagal transmission of hepatic energy state [71]. Previously, we observed reduced maximal liver MEM in LPGC1a+/− compared to WT mice under saturating substrate conditions [59]. Herein, we used a more robust technique to measure the capacity of isolated liver mitochondria to increase respiration in response to physiologically relevant changes in energy state (ΔG_{ATP}) (Figure 1A). Supporting our previous findings, liver mitochondria from LPGC1a+/− mice had reduced respiration of fatty acids at all ΔG_{ATP} levels tested. More importantly, LPGC1a+/− liver mitochondria had reduced capacity to increase respiration in response to changing energy demand (i.e., conductance - slope of line across ΔG_{ATP} states). To further investigate the impact of energy demand on WT and LPGC1a+/− liver MEM, we used overnight fasting/re-feeding as a systemic energy challenge to measure the adenine nucleotide pool (Figure 1B). LPGC1a+/− mice had lower liver ATP levels and increased AMP levels following the overnight fast, which were ameliorated by 4 h of re-feeding. Additionally, liver energy charge (Figure 1C)] and NAD^+/NADH ratio (Figure 1D) were reduced in fasted LPGC1a +/− mice. Importantly, no differences in total adenine nucleotide pool were observed between genotypes within the feeding conditions (Fig. S1A). However, total nicotinamide adenine nucleotide pool was increased in LPGC1a+/− liver during fasting (Fig. S1B), due to a large increase in NADH concentration (Fig. S1D). Notably, both genotypes experienced a similar level of energy pressure upon the liver as witnessed by the lack of difference during fasting for glycogen and gluconeogenic marker PEPCK mRNA expression [72,73] (Figure 2A and B). These findings demonstrate a reduced capacity of male LPGC1a+/− liver MEM to maintain ATP during changes in energy demand.

While reduced basal expression of liver mitochondrial respiratory and β-oxidation genes has been observed in LPGC1a+/− mice [59,60], how these hepatic transcriptional programs would respond to energy stress is not known. Therefore, we assessed mRNA expression of PGC1a and MEM genes in the fasted/refed liver samples. As expected, liver PGC1a expression was ∼50% reduced in LPGC1a+/− mice compared to WT during all phases of the fasting/re-feeding experiment (Figure 1E). Importantly, no genotype specific gene expression differences in PGC family members, PGC1b and PPRC1 were observed (Figure 1F,G), demonstrating a lack of compensatory expression. However, N-terminal PGC1a (NT-PGC1a) expression was approximately 50% lower under basal and refed conditions in LPGC1a+/− mice compared to WT (Figure 1H). While no difference in NT-PGC1a expression was observed between genotypes during fasting, fasted LPGC1a+/− mice had greater NT-PGC1a expression compared to basal and refed. Additionally, the primary PGC1a mitochondrial transcription factor targets, nuclear respiratory factor-1 (NRF1) [74], nuclear respiratory factor-2 (GABPA) [74], and mitochondrial transcription factor-a (TFAM) [75] were assessed. Only NRF-1 was observed to be different by genotype, with reduced expression under basal and fasted conditions in LPGC1a+/− mice (Figure 2D, E & F, respectively). Also, markers of liver mitochondrial content were assessed. While Cox IV nuclear subunit, Cox4i2, expression was increased by fasting in WT and tended to be higher compared to LPGC1a (Figure 1I), liver citrate synthase activity was not affected by genotype or fasting/refeeding (Fig. S2C).

PGC1a was discovered as a transcriptional co-regulator of PPARγ in brown adipose [76], and regulates hepatic lipid homeostasis and oxidative metabolism pathways [77]. Fasting increased liver expression of mitochondrial (HADHA) and peroxisomal (ACOX1) β-oxidation (Figure 1J & S2I, respectively), mitochondrial uptake of long-chain acyl-CoA (CPT1a, Fig. S2G), mitochondrial uncoupling protein 2 (UCP2, Fig. S2H), and ketone synthesis (HMGCS2, Figure 1K) genes in both genotypes. However, HADHA and HMGCS2 tended to have higher expression in WT compared to LPGC1a during fasting. PPARα mRNA

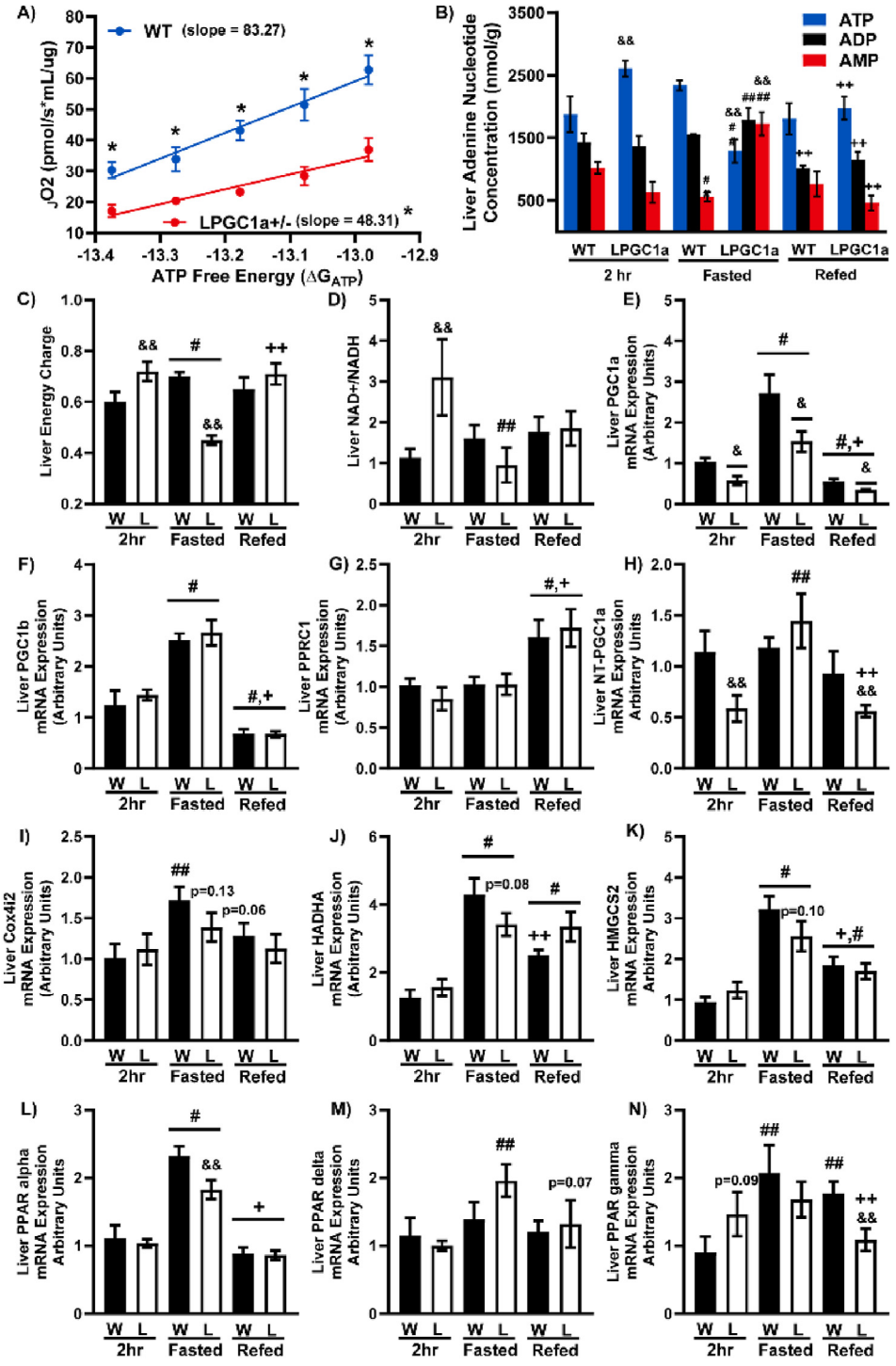

Figure 1: LPGC1a+/− LPGC1a+/− Mice Have Reduced ATP Homeostasis During Fasting. A) Respiration of isolated liver mitochondria during changes in ATP free energy (ΔG ATP) via creatine kinase clamp. B) Liver ATP, ADP, & AMP concentration (nmol/g) in mice after 2hr food withdrawal, 18 h fast, or 4 h refeeding. Impact of fasting/re-feeding on the liver was assessed as C) liver energy charge (ATP + (0.5 × ADP))/(ATP + ADP + AMP), D) NAD+/NADH, and mRNA expression of E) PGC1a, F) PGC1b, G) PPRC1, H) NT-PGC1a, I) Cox4i2, J) HADHA, K) HMGCS2, L) PPAR alpha, M) PPAR delta, and N) PPAR gamma in 2hr food withdrawn, 18hr fasted, or 4 h refed mice. Data are represented as mean ± SEM. n = 3–8 biological replicates for each genotype for adenine nucleotide concentration. For all other data, n = 8–10 biological replicates for each genotype. For Figure 1A, *p < 0.05 between genotypes within ATP free energy state by two sample t-test. For Figure 1B–N, two-way ANOVA – Main Effects: & p < 0.05 genotype, #p < 0.05 fasting or refeeding compared to 2hr, + p < 0.05 refed vs fasted. Fisher's LSD *post-hoc*: ## fasting versus 2 h within genotype, && LPGC1a+/− versus wildtype within fed state, and ++ refed versus fasting within genotype. See Fig. S1 for additional liver adenine nucleotide data and Fig. S2 for additional liver mRNA expression of mitochondrial genes in 2hr food withdrawn, fasted, and 4 h refed mice.

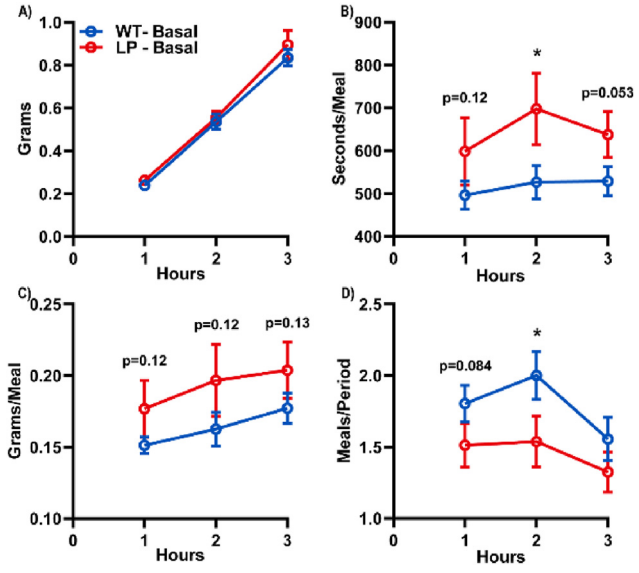

Figure 2: Reduced Liver-Specific PGC1a Results in Underlying Differences in Feeding Behavior. A) Acute basal food intake at the beginning of the dark cycle following 2hr food withdrawal. B) Average number of meals, C) grams per meal, and D) length of each meal during each 1hr period. Data are represented as mean ± SEM. n = 13 technical replicates and n = 7–9 biological replicates for each genotype. *p < 0.05 between genotypes within time point by two sample t test.

was reduced in LPGC1a+/− mice compared to WT during fasting (Figure 1L), while PPARδ was increased by fasting in the LPGC1a+/− mice, but not WT (Figure 1M). Also, liver PPARγ expression tended to be higher in LPGC1a+/− under basal conditions (Figure 1N), but was increased by fasting only in WT mice. Finally, PGC1a-targeted regulation of hepatocyte mitochondria and gluconeogenic transcription factors, hepatocyte nuclear respiratory factor 4a (HNF4a) and forkhead box O1 (FOXO1), was not different between genotypes regardless of condition (Figure 2J and K, respectively). Together, these data suggest a modest diminished liver transcriptional response to energy stress in male LPGC1a+/− mice, impacting maintenance of liver MEM and energy state.

Recent work demonstrated that hepatocyte membrane potential is involved in a modulation of vagal signaling linking peripheral energy metabolism and central regulation of metabolism, including food intake [78,79]. The primary component responsible for hepatocyte membrane potential maintenance is the action of the Na/K-ATPase, which represents up to ∼35% of hepatocyte energy utilization [80]. Interestingly, fasting generates increased liver mRNA expression of Na/K-ATPase components in WT mice (Fig. S3A–D). However, LPGC1a+/− mice had a smaller increase in the primary catalytic subunit (ATP1a1) and no changes in a regulatory subunit (FXYD1). To our knowledge, this is the first data demonstrating changes in hepatic expression of Na/K-ATPase subunits by energy stress or PGC1a expression. These findings suggest transcriptional responses to energy demand may play a role in the maintenance of hepatocyte ion gradients during the fasted to fed transition [81].

Together these data demonstrate hepatic PGC1a expression plays a unique role in the regulation of liver MEM functional and transcriptional pathways. Further, it demonstrates that the livers of male LPGC1a+/− mice lack the capacity to respond to physiologically relevant energy stress to maintain tissue ATP levels.

3.2. Reduced Liver-Specific PGC1a results in impaired satiation

Previously, we observed no differences in low-fat diet food intake and body weight in LPGC1a+/− mice compared to WT [59], however, whether feeding behavior was different was not assessed. Herein, no difference in cumulative chow intake in the first 3 h of the dark cycle is observed (Figure 2A). However, LPGC1a+/− mice had longer meals at 2 h (Figure 2B), tended to have larger meal size (Figure 2C), and consumed fewer meals at 2hrs (Figure 2D). These data suggest an association between reduced hepatic MEM and impaired within meal satiation, and further suggest that these underlying impairments in within meal satiation require increased dietary energy density to elicit greater food intake.

3.3. Male LPGC1a+/− mice are less sated by a mixed macronutrient gastric preload

Based on the previously observed increase in high-fat diet-induced food intake [59] and the underlying difference in meal pattern structure (Figure 2), we assessed whether reduced liver MEM impaired the food intake suppressive effects of oral mixed nutrient preloads. Oral gavage of 5, 10, and 15 mL/kg Ensure (5 kcal/mL) resulted in inhibition of chow intake in both genotypes (Figure 3A–C, M–O), with LPGC1a+/− mice having impaired suppression of food intake at all three doses compared to WT. Similar to Figure 2, LPGC1a+/− mice had increased meal duration (Figure 3E–G) and size (Figure 3I–K) during the different oral preload doses. However, no differences were observed in the number of meals between genotypes except at the highest dose (Fig. S4A–C). The inhibition of food intake by oral gavage of a mixed meal is due to satiation signals elicited by nutrients and distention of the GI tract. To assess whether food intake inhibition via mechanical distention of the GI tract was impaired in LPGC1a+/− mice, we administered non-nutritive methylcellulose oral pre-loads. Oral gavage of a 1% methylcellulose solution inhibited food intake to a greater extent in WT mice compared to LPGC1a+/− (Figure 3D). However, this was not due to significant differences in meal duration (Figure 3H), size (Figure 3L), or number (Fig. S4D) as was observed with mixed nutrient. Further, a dose dependence of non-nutritive mechanical food intake inhibition was observed as an oral preload of 2% methylcellulose resulted in the same food intake inhibition in both genotypes (Fig. S4E–H). These data demonstrate that mice with reduced liver MEM have impaired meal termination in response to GI-derived satiation signals initiated by oral nutrients and mechanical distention.

3.4. Decreased Satiation Response in male LPGC1a+/− mice following gastric delivery of individual macronutrients

GI delivery of carbohydrate, protein, and lipids produces acute suppression of food intake in mice and humans (reviewed [6,17]). Therefore, we tested whether acute food intake inhibition by the individual macronutrients was reduced in LPGC1a+/− mice. One hour food intake inhibition following oral gavage of glucose was lower in LPGC1a+/− mice (Figure 4A) and tended to be lower following lipid and protein delivery (Figure 4B,C). Only protein tended to show a reduction of food intake inhibition in LPGC1a+/− across the data collection. Overall, feeding behavior differences were more subtle for the individual macronutrients. Following glucose oral pre-load, meal duration and size was greater at 3 h and tended to be greater at 1hr in LPGC1a+/− mice (Figure 4D,G), while lipid tended to increase LPGC1a+/− meal duration at 1 & 3 h (Figure 4E) and increased meal size at 1hr (Figure 4H). Protein increased meal duration and size at 2 h in LPGC1a+/− mice (Figure 4F,I). Number of meals following the three

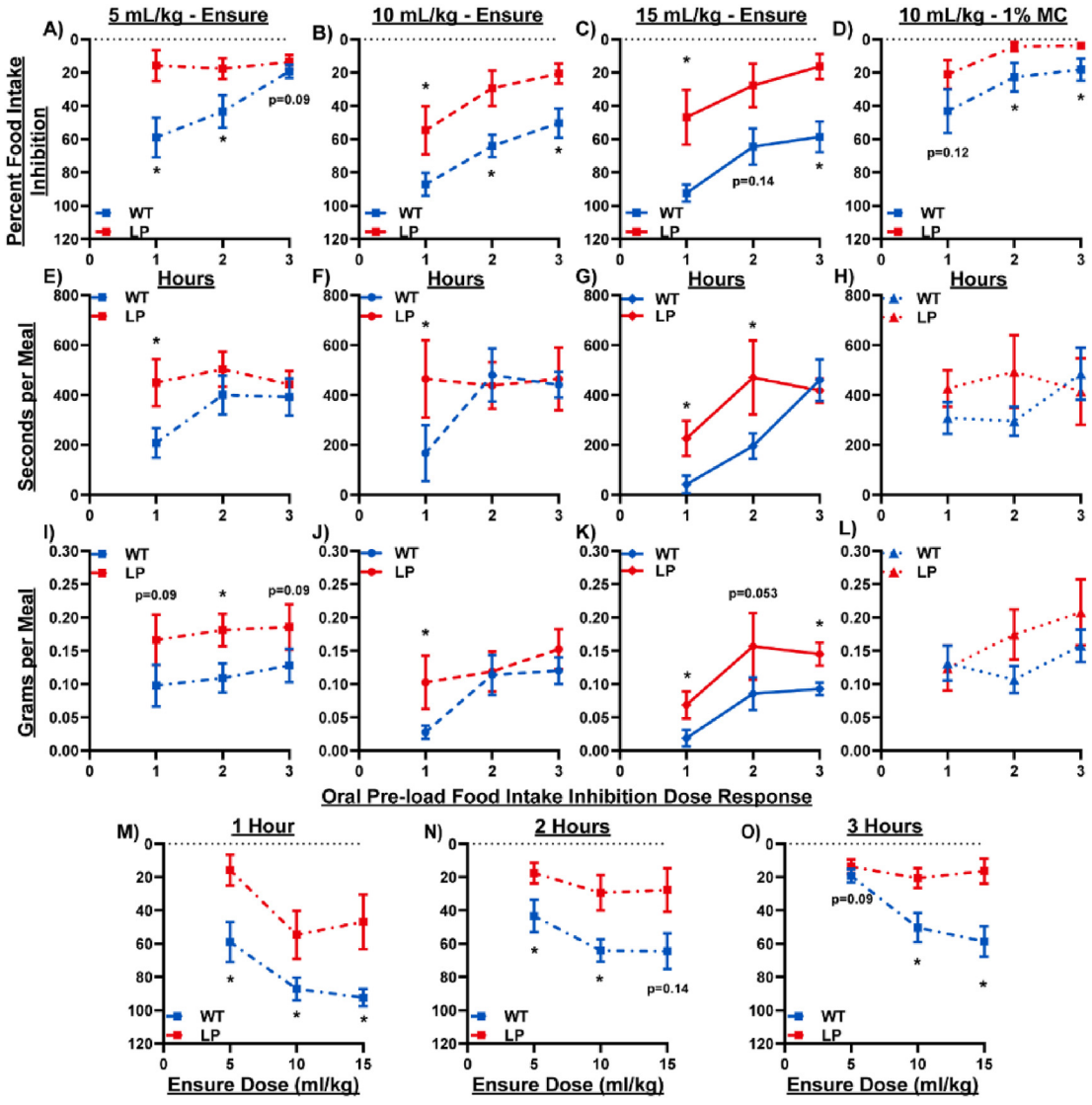

Figure 3: Dose Dependent Impairment in Satiation Following Mixed Macronutrient Oral-Preloads in LPGC1a+/− Mice. Percent inhibition of food intake following oral pre-load of Ensure® at A) 5, B) 10, & C) 15 mL/kg and D) 10 mL/kg 1% methylcellulose. Average duration of meal following mixed nutrient E) 5, F) 10, & G) 15 mL/kg, and H)10 m/kg methylcellulose oral pre-load. Average meal size following I) 5, J) 10, & K) 15 mL/kg nutrient, or L) 10 mL/kg non-nutritive oral pre-load. Ensure® oral pre-load food intake inhibition dose response at M) 1 h, N) 2 h, & O) 3 h. Data are represented as mean ± SEM. n = 7–9 biological replicates for each genotype. *$p < 0.05$ between genotypes within time point by two sample t test. See also Fig. S4 for meals per period data across the 3 oral pre-load doses.

macronutrients was not different, except glucose with LPGC1a+/− mice consuming fewer meals at 2 & 3 h (Fig. S5). These data demonstrate the impaired satiation observed in male LPGC1a+/− mice is not specific to a macronutrient.

3.5. Peripheral satiation signal receptor inhibition does not increase food intake following oral pre-loads in male LPGC1a+/− mice

From the above data, it is not possible to discern if a specific satiation signaling pathway is involved in the observed impairments in food intake inhibition. Therefore, we assessed whether peripheral serotonin (5HT), cholesystekinin (CCK-8), and glucagon-like peptide-1 (GLP-1) signaling pathways were impaired in the regulation of LPGC1a+/− mouse food intake inhibition (Figure 5A,B, & C, respectively). Peripheral delivery of receptor antagonists for 5-HT3R, CCK-1R, and GLP-1R robustly increased food intake in WT mice at following mixed nutrient oral preload. While 5-HT3R antagonism modestly increased LPGC1a+/− food intake following oral preload in LPGC1a+/− mice, CCK-1R and GLP1R blockade had little to no effect on food intake. Importantly, no difference in serum concentration of 5-HT, CCK-8S, or GLP-1(7–36) were observed between WT and LPGC1a+/− mice 60 min after mixed nutrient oral gavage (Fig. S6A–C). These findings suggest that the male LPGC1a+/− impairment in food intake inhibition is due to diminished or modulated vagal afferent satiation signaling rather than decreased release of meal derived GI-satiation signals.

3.6. Fasting Produces Greater Increases in Acute Food Intake in male LPGC1a+/− mice

Acute chemical reduction of liver ATP levels stimulates food intake [38,39,50–52], via the common hepatic branch vagus [38,39]. We tested whether the hepatic energy stress of fasting impacted acute food intake in differently LPGC1a+/− and WT mice. Fasted WT mice

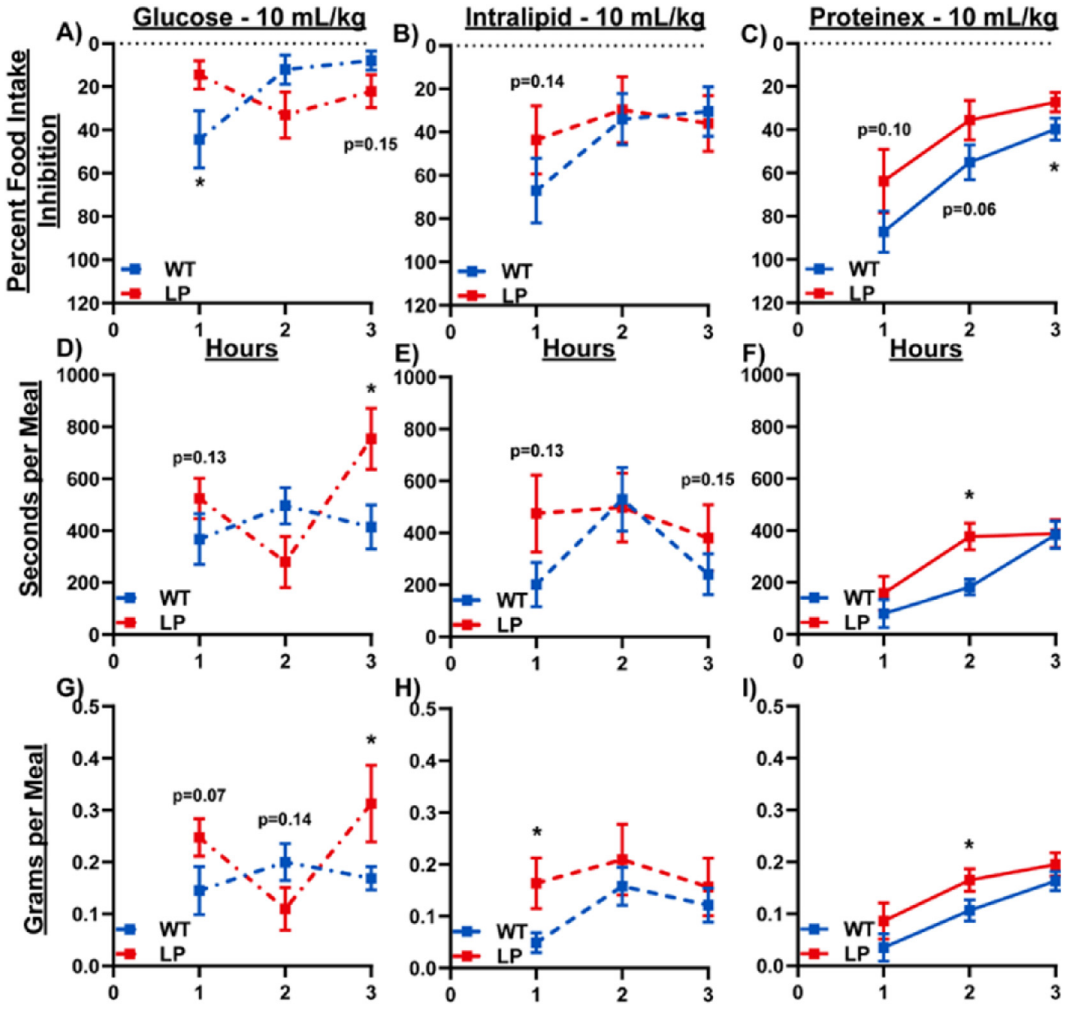

Figure 4: Decreased Satiation Response in LPGC1a+/− Mice Following Oral Delivery of Individual Macronutrients. Percent inhibition of food intake following oral pre-load of individual macronutrients at 10 mL/kg: A) 40% Glucose, B) Intralipid®, & C) Proteinex®. Average duration of meal following D) 40% Glucose, E) Intralipid®, & F) Proteinex® individual macronutrient oral pre-load. Average meal size following G) 40% Glucose, H) Intralipid®, & I) Proteinex® nutrient oral pre-load. Data are represented as mean ± SEM. n = 7–9 biological replicates for each genotype. *p < 0.05 between genotypes within time point by two sample t test. See also Fig. S5 for meals per period data across the 3 individual macronutrient oral pre-loads.

increased food intake 6.6-fold in the first 30 min compared to basal experiments (Figure 6A). However, LPGC1a+/− mice had 16.5-fold greater acute food intake compared to basal, and tended to have twice the increase compared to fasted WT mice. In both genotypes this increase was due to increased meal size, duration, number in both genotypes over basal in the first 30 min (Figure 6B–D). However, LPGC1a+/− mice increased meal size by 13.5-fold over basal, while WT mice increased meal size by only 3-fold. Further, LPGC1a+/− mice continued to have larger meal size (>2.5 fold) during the following 30-minute period. No genotype difference was observed for meal duration or number in this time period (Figure 6C,D). Also, LPGC1a+/− fasting-induced food intake was not as sensitive to peripheral satiation signal inhibition [i.e., CCK-8S (10 μg/kg)] compared to WT (Figure 6E,F). While these findings are striking, it must be noted that no difference in control meal size or meal duration were observed in this cohort of mice, unlike the previous findings above (Figure 2). Together, these findings demonstrate that the LPGC1a+/− mice have exaggerated acute food intake following an overnight fast, mainly through the consumption of larger meals.

3.7. Maladaptive Response of Hypothalamic POMC and AgRP expression to fasting in male LPGC1a+/− mice

Orexigenic AgRP/NPY and anorexigenic POMC neurons of the arcuate nucleus are central to the homeostatic regulation of food intake, with fasting serving as a powerful modulator of their expression. WT mice were observed to have a decrease in POMC during fasting and subsequent increase following re-feeding (Figure 7A). Interestingly, POMC expression was lower in LPGC1a+/− mice under basal conditions and no change in expression was observed during either fasting or re-feeding. Importantly, AgRP expression was higher in LPGC1a+/− mice compared to WT during fasting (Figure 7B), while NPY expression was increased with fasting in WT but not LPGC1a+/− mice (Figure 7C). To assess whether these differences in expression were due to differences in AgRP or POMC neuron number, we measured the total area of POMC and AgRP expression in the arcuate nucleus by *in situ* hybridization after a 4-hour food withdrawal. POMC fluorescent area was reduced (Figure 7D) and AgRP increased (Figure 7E) in the LPGC1a+/− mice. While the increase in fasting-induced acute food intake in Figure 6 is consistent with increased mRNA expression of

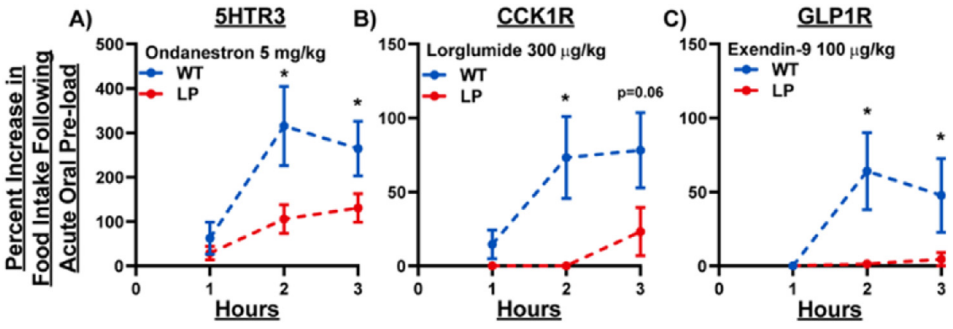

Figure 5: Peripheral Satiation Signal Receptor Inhibition Does Not Impact Food Intake Following Oral Pre-Loads in LPGC1a+/− Mice. Percent increase in chow intake during acute mixed nutrient oral pre-load (10 mL/kg) following intraperitoneal delivery of satiation signal receptor inhibitors A) Ondanestron (5HTR3 antagonist, 5 mg/kg), B) Lorglumide (CCK1R antagonist, 300 μg/kg), and C) Exendin-9 (GLP1R antagonist, 100 μg/kg). Data are represented as mean ± SEM. n = 7–9 biological replicates for each genotype. *p < 0.05 between genotypes within time point by two sample t test.

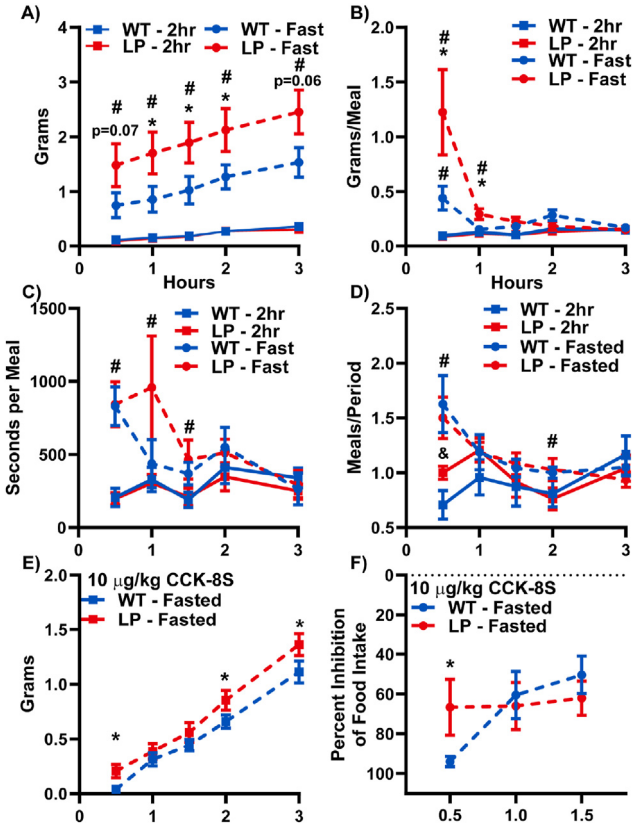

Figure 6: Fasting Produces Greater Increases in Acute Food Intake in LPGC1a+/− Mice. A) Cumulative food intake, B) grams/meal per 0.5 h period, C) meals per period, and D) seconds per meal in WT and LPGC1a+/− mice fasted for 18 h compared to 2hr food withdrawal. E) Cumulative food intake and F) percent inhibition of food intake in 18hr fasted mice receiving 10 μg/kg CCK-8S prior to access to food. Data are represented as mean ± SEM. n = 7–9 biological replicates for each genotype. *p < 0.05 between genotypes within fasting and time point, & p < 0.05 between genotypes within 2hr food withdrawal and time point, and #p < 0.05 between treatment within genotype and time point by two sample t test.

AgRP in the hypothalamus of LPGC1a+/− mice, the basal *in situ* hybridization findings may suggest differences in neuron number between WT and LPGC1a+/− mice. Together, fasting reduces liver ATP, increases hypothalamic orexigenic gene expression, and elevates acute food intake in male LPGC1a+/− mice.

4. DISCUSSION

In the 1960s, Russek first suggested that liver metabolism could serve as a sensor in the peripheral regulation of food intake [36,82–84]. Subsequently, Langhans and Friedman independently reported vagal afferent communication of liver MEM to higher neural structures as a mediator of food intake. These studies chemically blocked fatty acid oxidation (FAO) [41–43,47–49] and/or lowered ATP levels [38,39,50–53] which increased acute food intake, altered meal patterns [44,85], and was hypothesized to decrease vagal afferent activation in rodents [39,40,86–88]. Furthermore, common hepatic branch vagotomy or chemical deafferentation prevented the effects of reduced ATP or FAO [37–40,89,90]. However, it was later proposed that sensing of small intestine FAO, not hepatic, was involved in peripheral food intake regulation [91,92]. This new premise, combined with the debate regarding vagal afferent innervation of the liver parenchyma [93] and the reduced rigor of intraperitoneal chemical inhibition and vagotomy experiments, reduced interest in the study of liver MEM as a mediator of food intake. However, numerous contemporary findings, coupled with major technological advancements, have revived the hypothesis that liver MEM can modulate vagal afferent sensory neuron signaling impacting energy homeostasis [59,94–96] and metabolic disease development and progression [78,79,97–100]. Specifically, recent findings show that hepatic vagal afferent signals are required for the development of diet-induced steatosis [101] and the circadian regulation of food intake [102]. Herein, we report impaired food intake inhibition following oral nutrient pre-load and greater fasting-induced food intake in a mouse model with decreased hepatocyte MEM (e.g., oxidative metabolism [59], respiratory function, adaptability to changes in energy demand, and ATP homeostasis). These food intake phenotypes were characterized by greater within meal food intake and meal length, suggesting impaired GI-derived satiation signaling. In support of compromised satiation signaling, peripheral antagonism of vagal afferent satiation signal receptors failed to increase relative food intake following oral nutrient pre-load, and peripheral exogenous satiation signal delivery did not strongly inhibit fasting-induced food intake.

A large body of work shows that altered liver mitochondrial oxidative metabolism and ATP homeostasis is associated with obesity. In human subjects with obesity, liver ATP concentration is inversely proportional to BMI [103–105], waist-to-hip ratio [106,107], and hepatic lipid content [103]. Importantly, obesity drives compensatory responses in hepatic oxidative metabolism [108], including increased TCA flux [109–111]. However, these adaptations do not protect liver ATP

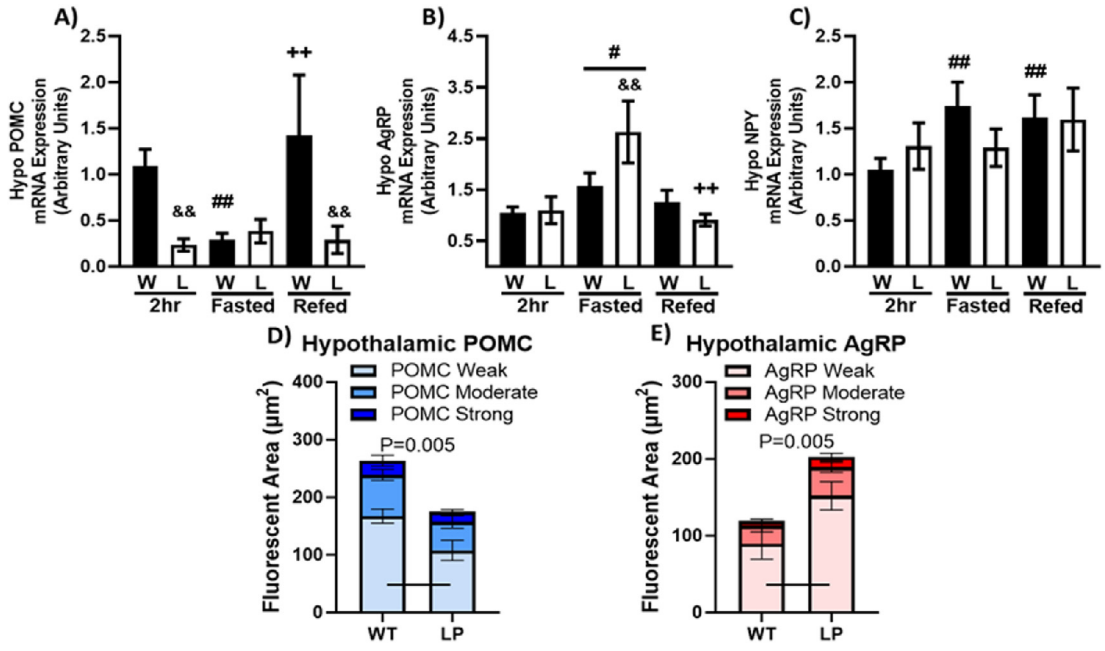

Figure 7: Maladaptive Response of Hypothalamic POMC and AgRP Expression to Fasting in LPGC1a+/− Mice. Gene expression of A) POMC, B) AgRP, and C) NPY in the hypothalamus of 2hr food withdrawn, fasted, and 4 h refed mice. *In situ* hybridization of D) POMC and E) AgRP in the arcuate nucleus of the hypothalamus of 2hr food withdrawn wildtype and LPGC1a+/− mice. Data are represented as mean ± SEM. n = 8–10 biological replicates for each genotype. # main effect fasting compared to 2hr by two-way ANOVA (B). ## fasting versus 2 h within genotype, && LPGC1a+/− versus wildtype within group, and ++ refed versus fasting within genotype pairwise comparisons were performed using Fishers LSD (A, B, & C). D) and E) genotyped compared by two sample t test. Representative fluorescent *in situ* hybridization images from analysis of the total area of POMC and AgRP expression are presented in Fig. S8.

homeostasis in obese individuals as observed by reduced basal or fasting hepatic ATP concentration [104,107,112], ATP recovery rate [104,113–115], and poor coupling of mitochondrial oxygen consumption to ATP synthesis (as respiratory control ratio) [116]. This reduction in human hepatic ATP homeostasis is due in part to decreased electron transport system (ETS) complex activities [116], complete FAO to CO_2 [117], mitochondrial turnover [117], and mitochondrial entry of long-chain fatty acids in subjects with obesity [108]. Similarly, DIO rodents demonstrate decreased liver complete FAO [55,118,119], mitochondrial FFA respiration [55,70,120], reduced expression and activity of ETS complexes [121–129], increased NADH/NAD + ratios [78,122,123], and impaired capacity to maintain hepatic ATP levels [122–125,130]. In humans and rodents, these impairments in hepatic MEM are associated with decreased expression of the mitochondrial co-transcriptional regulator, peroxisomal proliferator-activated receptor γ co-activator 1α (PGC1a) [112,116,122–124,126,130–137], as well as, its transcriptional targets involved in mitochondrial transcription pathways: mitochondrial transcription factor-a (TFAM) [127,130,132,133] and nuclear respiratory factor-1 [130,132]. Importantly, the male LPGC1a+/− mouse model recapitulates the MEM pathophysiologies of reduced PGC1a and NRF1 expression (Figure 1E & S2D), decreased mitochondrial complete FAO [59] and FFA respiration (Figure 1A), increased NADH/NAD + ratio (Figure 1D), and impaired ATP homeostasis (Figure 1B), without the potential confounding influence of obesity. Further, the mitochondrial respiration findings in Figure 1A build upon our previous work by demonstrating that the reduced liver MEM of LPGC1a+/− mice is characterized by an impaired capacity to increase respiration in response to increasing energy demand. Additionally, this model replicates the reduced liver MEM of earlier food intake studies [37–44,47–53,85–90], while more specifically targeting the liver, specifically hepatocytes. All told, the association of impaired hepatic ATP homeostasis and reduced satiation [19–31] observed in obesity, implicates liver ATP homeostasis as a potential regulator of the interoceptive processes controlling within-meal food intake inhibition. Previously, we have observed increased acute high-fat diet-induced food intake and weight gain in animals with chronically reduced liver MEM [55–57]. Alternatively, elevated hepatic FAO via CPT1a overexpression decreased food intake during chronic high-fat diet feeding [138]. Further, increased liver glucose flux resulted in decreased weight gain, increased vagal-mediated food intake inhibition, and increased orexigenic gene expression in the hypothalamus [94–96]. As described above, early data implicated liver MEM in the regulation of food intake via modulation of vagal afferent neuron signaling through chemical inhibition of liver fatty acid oxidation and/or ATP depletion [37,39–42,48,49,51,52,54,86–88,90]. As mentioned, male LPGC1a+/− mice have increased short-term high-fat diet food intake, larger meal size, and greater weight gain compared to WT littermates [59]. Importantly, no differences were observed in food intake or weight gain between LPGC1a+/− and WT mice on low-fat diet. While the increased high-fat diet food intake and meal size suggested impaired food intake regulation, the pathophysiology was unknown. In the current study, we observed LPGC1a+/− mice have underlying differences in meal size, duration, and number without differences in food intake during normal chow feeding (Figure 2). Further, we observed reduced liver MEM in LPGC1a+/− mice was associated with decreased dose-dependent food intake inhibition by oral pre-loads of mixed macronutrients and non-nutritive methylcellulose (Figure 3). Importantly, greater meal size and duration were associated with the decreased mixed nutrient food intake inhibition of the LPGC1a+/− mice, phenotypes not observed during non-nutritive oral pre-loads. Supporting a role of reduced nutrient-induced, GI-derived satiation

signaling in the impaired food intake inhibition of the male LPGC1a+/− mouse. Further, male LPGC1a+/− mice had reduced food intake inhibition following oral gavage of individual macronutrients (Figure 4). These data were not as striking as those observed with mixed macronutrient, which is potentially a consequence of the reduced caloric density of the oral nutrient pre-loads at the 10 mL/kg dose (∼0.6 kcal − lipid & protein, ∼0.48 kcal − glucose, compared to ∼1.5 kcal of Ensure). However, these findings suggest that the energy density of the nutrient loads may be involved in eliciting a stronger phenotype. Also, this could explain why the only the high-fat diet fed male LPGC1a+/− mice had greater within meal food intake in our previous work [59]. Additional, support for reduced liver MEM impairing nutrient-induced, GI-derived satiation in LPGC1a+/− mice, comes from the lack of increased food intake following antagonism of peripheral GI-derived satiation signal receptors (Figure 5). Further, the reduced fasting-induced liver ATP of LPGC1a+/− mice resulted in a dramatic increase in acute food intake and meal size (Figure 6). An increase that represented consuming over 25% of their daily food intake in 30 min, compared to ∼2% under basal conditions. Also, this increased acute food intake was only modestly inhibited by a relatively large satiation signal dose (10 μg/kg CCK-8S). To our knowledge this is the first data showing the potential role of liver MEM and ATP homeostasis on within meal feeding behavior and food intake inhibition by nutrient-induced, GI-derived signals.

Collectively, our findings suggest a role for liver MEM in the interoceptive control of meal termination by GI-derived satiation signals. Appropriate meal termination requires higher order brain structures to integrate neuroendocrine signals initiated by gastric distension and gut-derived neuropeptides/neurotransmitter activation of vagal afferent neurons (reviewed in [139–142]). The modulation of these neural signals by peripheral energy metabolism could serve as a mechanism to communicate peripheral tissue energy state to the brain. Recently, Geisler et al. proposed that reduced hepatic ATP lowers Na/K-ATPase activity, resulting in hepatocyte membrane depolarization, increased GABA secretion, and inhibition of vagal afferent firing [78,79]. As described above, liver ATP levels are reduced in human subjects and rodent models with obesity. Additionally, liver Na/K-ATPase activity is reduced in diet-induced obese rodents [143], and IP delivery of ouabain (Na/K-ATPase inhibitor) increases food intake [144]. Further, chemical inhibition of fatty acid oxidation [145], Na/K-ATPase activity [146–149], ATP depletion [148], and electrogenic nutrient uptake [150] depolarizes primary hepatocytes. Classically, the liver is considered a primary site of peripheral GABA degradation through GABA-transaminase and the GABA shunt, as such, hepatocytes express four GABA transporters which are involved in sodium-dependent GABA uptake [151]. However, the equilibrium constant of GABA-transaminase favors GABA synthesis [152]. Hepatocyte GABA synthesis through GABA-T would be favored through the low liver NAD+/NADH observed in fasted LPGC1a+/− mice (Figure 1D) and obese models [78,122,123]. As such, GABA secretion is increased in obese mouse liver sections and following inhibition of Na/K-ATPase [78]. Finally, using hepatocyte-specific expression of a ligand-gated sodium channel, the authors demonstrated real-time reductions in vagal afferent firing rate and hepatocyte membrane depolarization during ligand application [78]. The maintenance of hepatocyte membrane potential by ATP-dependent Na/K-ATPase activity represents ∼35% of hepatocyte oxygen consumption [80]. As such, any reduction in liver ATP homeostasis could lead to hepatocyte membrane depolarization and reduced vagal afferent communication of peripheral satiation signals. Our observations of increased acute meal size (Figure 6B) and impaired CCK inhibition of food intake (Figure 6F) in fasted LPGC1a+/− mice with reduced liver ATP supports this speculation. In hepatocytes, the Na/K-ATPase is primarily comprised of the ATP1a1 catalytic subunit, either ATP1b1 or ATP1b3 subunit, and the FXYD1 regulatory subunit (reviewed [153,154]). Our observation of fasting-induced increases in hepatic Na/K-ATPase subunit gene expression (Figure 3 A-F), represent the first report of energy stress impacting transcriptional regulation of these genes. Further, the reduction in fasting-induced expression of the ATP1a1 catalytic subunit (Fig. S3A) and FXYD1 regulatory subunit (Fig. S3D) implicate PGC1a in the regulation of hepatocyte Na/K-ATPase function and membrane potential. While speculative, these data suggest impaired capacity to maintain membrane potential in male LPGC1a+/− mouse during challenges to ATP homeostasis. Future work will focus on the role of impaired hepatocyte mitochondrial ATP homeostasis on the function of the Na/K-ATPase system, maintenance of the cellular membrane potential, and experiments on the role of hepatocyte membrane polarization state in meal termination by GI-derived satiation signals.

A minor number of limitations require consideration in the interpretation and translation of our findings. First, the liver has been shown to secrete a growing number of factors, hepatokines, many of which are regulated by fasting/re-feeding and/or regulate food intake [155]. While beyond the scope of this manuscript, we assessed the gene expression of 6 hepatokines thought to be involved in food intake regulation in fasted/re-fed WT and LPGC1a+/− mice (Fig. S7). Only FGF21 expression tended to be lower in LPGC1a+/− mice during fasting ($p = 0.12$). While liver FGF21 expression has been observed to be increased in fasting, it's role in food intake regulation has been refined to increased preference of protein and inhibition of carbohydrate consumption [155]. Although we have observed similar FGF21 serum levels in WT and LPGC1a+/− mice [156], future experiments may investigate a potential role of reduced fasting liver FGF21 expression in acute food intake inhibition. Second, our previous work we did not observe differences in diet-induced weight gain or high-fat diet food intake in female wildtype and LPGC1a+/− mice [59]. While this is why we have focused on males to this point, we are unable to discuss the role of sex on liver MEM and food intake regulation. Future work will include female groups to assess if liver MEM is involved in the previously observed phenotypes. Finally, limitations of the rigor of the modeling system must be considered. Hepatocyte PGC1a co-regulates other transcriptional pathways beyond mitochondrial bioenergetics, particularly, gluconeogenesis, antioxidant, and anti-inflammatory pathways [77]. As such, it is possible that changes in these transcriptional pathways in hepatocytes are influencing the observed food intake regulation phenotypes. Although, LPGC1a+/− mice had normal fasting/refed regulation of PEPCK expression (Fig. S2B), suggesting gluconeogenic activity was not altered. Additionally, limited data suggests that albumin is expressed in non-hepatic tissues [157,158], which would impact the tissue-specificity of the PGC1a heterozygosity. Further, expression of albumin-*cre* recombinase begins approximately halfway through gestation (∼10.5 of 20 day gestation [159]), potentially resulting in developmental changes that impact adult metabolic physiology. This is supported by the findings that offspring of high-fat fed dams have decreased liver PGC1a expression [160,161], increased AgRP/NPY and decreased POMC hypothalamic expression [162], and our *in situ* hybridization data in Figure 7. Future experiments will be performed in adult-onset models with more targeted genetic alterations using hepatocyte-specific delivery of *cre* recombinase via AAV to more specifically model reductions in hepatocyte mitochondrial ATP homeostasis.

CONCLUSIONS

In summary, we demonstrate that decreased liver MEM alters feeding microstructure and food intake inhibition in response to nutrients. In combination with others [78,79], these data support a novel interoceptive mechanism by which liver energy metabolism can modulate acute food intake through reduced vagal afferent activity due to increased hepatocyte GABA secretion secondary to impaired maintance of membrane potential. Experiments are ongoing to further investigate the capacity of hepatic mitochondrial energy metabolism and ATP homeostasis to modulate meal termination in male and female mice through 1) increased rigor and specificity of hepatic mitochondrial models, 2) assessment of hepatocyte membrane potential and GABA under conditions of reduced hepatocyte MEM, and 3) determination of food intake regulation during acute chemogenetic hepatocyte membrane potential manipulation. Future work will include confirming the necessity of vagal afferents in the regulation of food intake through transmission of reduced hepatocyte MEM, and identifying the vagal afferent and higher order neural populations involved.

ACKNOWLEDGEMENTS

The authors wish to thank David Wasserman for years of scientific mentoring, career advice, and comedy relief. You will be missed.

CRediT AUTHORSHIP CONTRIBUTION STATEMENT

Michael E. Ponte: Writing — review & editing, Writing — original draft, Methodology, Investigation, Formal analysis, Data curation. **John C. Prom:** Writing — review & editing, Writing — original draft, Methodology, Investigation, Formal analysis, Data curation. **Mallory A. Newcomb:** Writing — review & editing, Methodology, Investigation, Formal analysis, Data curation. **Annabelle B. Jordan:** Writing — review & editing, Methodology, Investigation, Formal analysis, Data curation. **Lucas L. Comfort:** Writing — review & editing, Methodology, Investigation, Formal analysis, Data curation. **Jiayin Hu:** Writing — review & editing, Methodology, Investigation, Formal analysis, Data curation. **Patrycja Puchalska:** Writing — review & editing, Methodology, Investigation, Formal analysis, Data curation. **Devin C. Koestler:** Writing — review & editing, Methodology, Formal analysis, Data curation. **Caroline E. Geisler:** Writing — review & editing, Supervision, Methodology, Formal analysis, Conceptualization. **Matthew R. Hayes:** Writing — review & editing, Supervision, Methodology, Formal analysis, Conceptualization. **E. Matthew Morris:** Writing — review & editing, Writing — original draft, Supervision, Methodology, Investigation, Formal analysis, Data curation, Conceptualization.

DECLARATION OF COMPETING INTEREST

The authors declare that they have no known competing financial interests or personal relationships that could have appeared to influence the work reported in this paper.

FUNDING

This work was facilitated by resources and equipment within the Metabolism and Cell, Tissues, Bioanalysis, and Bioinformatics Cores of the Kansas Center for Metabolism and Obesity Research COBRE (NIH P20GM144269). The following funding supported this work: NIH T32DK128770 (MEP), NIH F32DK127591 (CEG), NIH R01DK112812 (MRH), NIH K01DK112967 (EMM), NIH P20GM144269 (EMM), Kansas INBRE (P20GM103418), KUMC Research Institute Lied Basic Science Grant (EMM), KU Diabetes Institute Pilot Grant (EMM).

DATA AVAILABILITY

Data will be made available on request.

RESOURCE AVAILABILITY

Requests for further information and resources should be directed to and will be fulfilled by the lead contact, E. Matthew Morris (emorris2@kumc.edu).

APPENDIX A. SUPPLEMENTARY DATA

Supplementary data to this article can be found online at https://doi.org/10.1016/j.molmet.2025.102167.

REFERENCES

[1] Schachter S. Obesity and eating. Internal and external cues differentially affect the eating behavior of obese and normal subjects. Science 1968;161(3843):751—6.
[2] Woods SC. Gastrointestinal satiety signals I. An overview of gastrointestinal signals that influence food intake. Am J Physiol Gastrointest Liver Physiol 2004;286(1):G7—13.
[3] Berthoud HR. The neurobiology of food intake in an obesogenic environment. Proc Nutr Soc 2012;71(4):478—87.
[4] Smith GP. The controls of eating: a shift from nutritional homeostasis to behavioral neuroscience. Nutrition 2000;16(10):814—20.
[5] Simmons WK, DeVille DC. Interoceptive contributions to healthy eating and obesity. Curr Opin Psychol 2017;17:106—12.
[6] Cummings DE, Overduin J. Gastrointestinal regulation of food intake. J Clin Investig 2007;117(1):13—23.
[7] Clemmensen C, Muller TD, Woods SC, Berthoud HR, Seeley RJ, Tschop MH. Gut-brain cross-talk in metabolic control. Cell 2017;168(5):758—74.
[8] Albaugh VL, He Y, Munzberg H, Morrison CD, Yu S, Berthoud HR. Regulation of body weight: lessons learned from bariatric surgery. Mol Metabol 2022:101517.
[9] Wang YB, de Lartigue G, Page AJ. Dissecting the role of subtypes of gastrointestinal vagal afferents. Front Physiol 2020;11:643.
[10] Berthoud HR, Albaugh VL, Neuhuber WL. Gut-brain communication and obesity: understanding functions of the vagus nerve. J Clin Investig 2021;131(10).
[11] Su Z, Alhadeff AL, Betley JN. Nutritive, post-ingestive signals are the primary regulators of AgRP neuron activity. Cell Rep 2017;21(10):2724—36.
[12] Goldstein N, McKnight AD, Carty JRE, Arnold M, Betley JN, Alhadeff AL. Hypothalamic detection of macronutrients via multiple gut-brain pathways. Cell Metab 2021;33(3):676—687 e675.
[13] Kupari J, Haring M, Agirre E, Castelo-Branco G, Ernfors P. An atlas of vagal sensory neurons and their molecular specialization. Cell Rep 2019;27(8):2508—2523 e2504.
[14] Bai L, Mesgarzadeh S, Ramesh KS, Huey EL, Liu Y, Gray LA, et al. Genetic identification of vagal sensory neurons that control feeding. Cell 2019;179(5):1129—1143 e1123.
[15] Beutler LR, Chen Y, Ahn JS, Lin YC, Essner RA, Knight ZA. Dynamics of gut-brain communication underlying hunger. Neuron 2017;96(2):461—475 e465.
[16] Powley TL, Phillips RJ. Gastric satiation is volumetric, intestinal satiation is nutritive. Physiol Behav 2004;82(1):69—74.
[17] Ritter RC. Gastrointestinal mechanisms of satiation for food. Physiol Behav 2004;81(2):249—73.

[18] Camilleri M. Peripheral mechanisms in appetite regulation. Gastroenterology 2015;148(6):1219—33.
[19] Cornier MA, Grunwald GK, Johnson SL, Bessesen DH. Effects of short-term overfeeding on hunger, satiety, and energy intake in thin and reduced-obese individuals. Appetite 2004;43(3):253—9.
[20] Nefti W, Chaumontet C, Fromentin G, Tome D, Darcel N. A high-fat diet attenuates the central response to within-meal satiation signals and modifies the receptor expression of vagal afferents in mice. Am J Physiol Regul Integr Comp Physiol 2009;296(6):R1681—6.
[21] Desai AJ, Dong M, Langlais BT, Dueck AC, Miller LJ. Cholecystokinin responsiveness varies across the population dependent on metabolic phenotype. Am J Clin Nutr 2017;106(2):447—56.
[22] Nauck MA, Vardarli I, Deacon CF, Holst JJ, Meier JJ. Secretion of glucagon-like peptide-1 (GLP-1) in type 2 diabetes: what is up, what is Down? Diabetologia 2011;54(1):10—8.
[23] Faerch K, Torekov SS, Vistisen D, Johansen NB, Witte DR, Jonsson A, et al. GLP-1 response to oral glucose is reduced in prediabetes, screen-detected type 2 diabetes, and obesity and influenced by sex: the ADDITION-PRO study. Diabetes 2015;64(7):2513—25.
[24] Covasa M, Ritter RC. Rats maintained on high-fat diets exhibit reduced satiety in response to CCK and bombesin. Peptides 1998;19(8):1407—15.
[25] Gourcerol G, Wang L, Wang YH, Million M, Tache Y. Urocortins and cholecystokinin-8 act synergistically to increase satiation in lean but not obese mice: involvement of corticotropin-releasing factor receptor-2 pathway. Endocrinology 2007;148(12):6115—23.
[26] Savastano DM, Covasa M. Adaptation to a high-fat diet leads to hyperphagia and diminished sensitivity to cholecystokinin in rats. J Nutr 2005;135(8):1953—9.
[27] de Lartigue G, Barbier de la Serre C, Espero E, Lee J, Raybould HE. Leptin resistance in vagal afferent neurons inhibits cholecystokinin signaling and satiation in diet induced Obese rats. PLoS One 2012;7(3):e32967.
[28] Duca FA, Sakar Y, Covasa M. Combination of obesity and high-fat feeding diminishes sensitivity to GLP-1R agonist exendin-4. Diabetes 2013;62(7):2410—5.
[29] Williams DL, Hyvarinen N, Lilly N, Kay K, Dossat A, Parise E, et al. Maintenance on a high-fat diet impairs the anorexic response to glucagon-like-peptide-1 receptor activation. Physiol Behav 2011;103(5):557—64.
[30] Mul JD, Begg DP, Barrera JG, Li B, Matter EK, D'Alessio DA, et al. High-fat diet changes the temporal profile of GLP-1 receptor-mediated hypophagia in rats. Am J Physiol Regul Integr Comp Physiol 2013;305(1):R68—77.
[31] Covasa M, Ritter RC. Reduced sensitivity to the satiation effect of intestinal oleate in rats adapted to high-fat diet. Am J Physiol 1999;277(1):R279—85.
[32] Daly DM, Park SJ, Valinsky WC, Beyak MJ. Impaired intestinal afferent nerve satiety signalling and vagal afferent excitability in diet induced obesity in the mouse. J Physiol 2011;589(Pt 11):2857—70.
[33] Rui L. Energy metabolism in the liver. Compr Physiol 2014;4(1):177—97.
[34] Wallimann T, Wyss M, Brdiczka D, Nicolay K, Eppenberger HM. Intracellular compartmentation, structure and function of creatine kinase isoenzymes in tissues with high and fluctuating energy demands: the 'phosphocreatine circuit' for cellular energy homeostasis. Biochem J 1992;281(Pt 1):21—40.
[35] Meffert G, Gellerich FN, Margreiter R, Wyss M. Elevated creatine kinase activity in primary hepatocellular carcinoma. BMC Gastroenterol 2005;5:9.
[36] Russek M. Participation of hepatic glucoreceptors in the control of intake of food. Nature 1963;197:79—80.
[37] Langhans W, Scharrer E. Evidence for a vagally mediated satiety signal derived from hepatic fatty acid oxidation. J Auton Nerv Syst 1987;18(1):13—8.
[38] Tordoff MG, Rawson N, Friedman MI. 2,5-anhydro-D-mannitol acts in liver to initiate feeding. Am J Physiol 1991;261(2 Pt 2):R283—8.
[39] Ritter S, Dinh TT, Friedman MI. Induction of Fos-like immunoreactivity (Fos-li) and stimulation of feeding by 2,5-anhydro-D-mannitol (2,5-AM) require the vagus nerve. Brain Res 1994;646(1):53—64.
[40] Horn CC, Tordoff MG, Friedman MI. Role of vagal afferent innervation in feeding and brain Fos expression produced by metabolic inhibitors. Brain Res 2001;919(2):198—206.
[41] Langhans W, Egli G, Scharrer E. Regulation of food intake by hepatic oxidative metabolism. Brain Res Bull 1985;15(4):425—8.
[42] Friedman MI, Tordoff MG. Fatty acid oxidation and glucose utilization interact to control food intake in rats. Am J Physiol 1986;251(5 Pt 2):R840—5.
[43] Scharrer E, Langhans W. Control of food intake by fatty acid oxidation. Am J Physiol 1986;250(6 Pt 2):R1003—6.
[44] Langhans W, Scharrer E. Role of fatty acid oxidation in control of meal pattern. Behav Neural Biol 1987;47(1):7—16.
[45] Friedman MI, Ramirez I, Bowden CR, Tordoff MG. Fuel partitioning and food intake: role for mitochondrial fatty acid transport. Am J Physiol 1990;258(1 Pt 2):R216—21.
[46] Rawson NE, Ulrich PM, Friedman MI. Fatty acid oxidation modulates the eating response to the fructose analogue 2,5-anhydro-D-mannitol. Am J Physiol 1996;271(1 Pt 2):R144—8.
[47] Del Prete E, Lutz TA, Althaus J, Scharrer E. Inhibitors of fatty acid oxidation (mercaptoacetate, R-3-amino-4-trimethylaminobutyric acid) stimulate feeding in mice. Physiol Behav 1998;63(5):751—4.
[48] Friedman MI, Harris RB, Ji H, Ramirez I, Tordoff MG. Fatty acid oxidation affects food intake by altering hepatic energy status. Am J Physiol 1999;276(4):R1046—53.
[49] Horn CC, Ji H, Friedman MI. Etomoxir, a fatty acid oxidation inhibitor, increases food intake and reduces hepatic energy status in rats. Physiol Behav 2004;81(1):157—62.
[50] Tordoff MG, Rafka R, DiNovi MJ, Friedman MI. 2,5-anhydro-D-mannitol: a fructose analogue that increases food intake in rats. Am J Physiol 1988;254(1 Pt 2):R150—3.
[51] Rawson NE, Blum H, Osbakken MD, Friedman MI. Hepatic phosphate trapping, decreased ATP, and increased feeding after 2,5-anhydro-D-mannitol. Am J Physiol 1994;266(1 Pt 2):R112—7.
[52] Rawson NE, Friedman MI. Phosphate loading prevents the decrease in ATP and increase in food intake produced by 2,5-anhydro-D-mannitol. Am J Physiol 1994;266(6 Pt 2):R1792—6.
[53] Koch JE, Ji H, Osbakken MD, Friedman MI. Temporal relationships between eating behavior and liver adenine nucleotides in rats treated with 2,5-AM. Am J Physiol 1998;274(3):R610—7.
[54] Kahler A, Zimmermann M, Langhans W. Suppression of hepatic fatty acid oxidation and food intake in men. Nutrition 1999;15(11—12):819—28.
[55] Morris EM, Jackman MR, Johnson GC, Liu TW, Lopez JL, Kearney ML, et al. Intrinsic aerobic capacity impacts susceptibility to acute high-fat diet-induced hepatic steatosis. Am J Physiol Endocrinol Metab 2014;307(4):E355—64.
[56] Matthew Morris E, Meers GM, Koch LG, Britton SL, MacLean PS, Thyfault JP. Increased aerobic capacity reduces susceptibility to acute high-fat diet-induced weight gain. Obesity 2016;24(9):1929—37.
[57] Morris EM, Meers GME, Ruegsegger GN, Wankhade UD, Robinson T, Koch LG, et al. Intrinsic high aerobic capacity in Male rats protects against diet-induced insulin resistance. Endocrinology 2019;160(5):1179—92.
[58] Wisloff U, Najjar SM, Ellingsen O, Haram PM, Swoap S, Al-Share Q, et al. Cardiovascular risk factors emerge after artificial selection for low aerobic capacity. Science 2005;307(5708):418—20.
[59] Morris EM, Noland RD, Ponte ME, Montonye ML, Christianson JA, Stanford JA, et al. Reduced liver-specific PGC1a increases susceptibility for short-term diet-induced weight gain in Male mice. Nutrients 2021;13(8).
[60] Estall JL, Kahn M, Cooper MP, Fisher FM, Wu MK, Laznik D, et al. Sensitivity of lipid metabolism and insulin signaling to genetic alterations in hepatic peroxisome proliferator-activated receptor-gamma coactivator-1alpha expression. Diabetes 2009;58(7):1499—508.
[61] Fisher-Wellman KH, Davidson MT, Narowski TM, Lin CT, Koves TR, Muoio DM. Mitochondrial diagnostics: a multiplexed assay platform for

comprehensive assessment of mitochondrial energy fluxes. Cell Rep 2018;24(13):3593–3606 e3510.
[62] Fisher-Wellman KH, Neufer PD. Linking mitochondrial bioenergetics to insulin resistance via redox biology. Trends Endocrinol Metabol 2012;23(3):142–53.
[63] Stagg DB, Gillingham JR, Nelson AB, Lengfeld JE, d'Avignon DA, Puchalska P, et al. Diminished ketone interconversion, hepatic TCA cycle flux, and glucose production in D-beta-hydroxybutyrate dehydrogenase hepatocyte-deficient mice. Mol Metabol 2021;53:101269.
[64] Fu X, Deja S, Kucejova B, Duarte JAG, McDonald JG, Burgess SC. Targeted determination of tissue energy status by LC-MS/MS. Anal Chem 2019;91(9):5881–7.
[65] Aschenbach WG, Hirshman MF, Fujii N, Sakamoto K, Howlett KF, Goodyear LJ. Effect of AICAR treatment on glycogen metabolism in skeletal muscle. Diabetes 2002;51(3):567–73.
[66] Larsen S, Nielsen J, Hansen CN, Nielsen LB, Wibrand F, Stride N, et al. Biomarkers of mitochondrial content in skeletal muscle of healthy young human subjects. J Physiol 2012;590(14):3349–60.
[67] Carabelli J, Burgueno AL, Rosselli MS, Gianotti TF, Lago NR, Pirola CJ, et al. High fat diet-induced liver steatosis promotes an increase in liver mitochondrial biogenesis in response to hypoxia. J Cell Mol Med 2011;15(6):1329–38.
[68] Srere PA. Citrate synthase. Methods Enzymol 1969;13:3–11.
[69] Morris EM, Meers GM, Booth FW, Fritsche KL, Hardin CD, Thyfault JP, et al. PGC-1alpha overexpression results in increased hepatic fatty acid oxidation with reduced triacylglycerol accumulation and secretion. Am J Physiol Gastrointest Liver Physiol 2012;303(8):G979–92.
[70] Morris EM, Jackman MR, Meers GM, Johnson GC, Lopez JL, MacLean PS, et al. Reduced hepatic mitochondrial respiration following acute high-fat diet is prevented by PGC-1alpha overexpression. Am J Physiol Gastrointest Liver Physiol 2013;305(11):G868–80.
[71] Friedman MI. An energy sensor for control of energy intake. Proc Nutr Soc 1997;56(1A):41–50.
[72] She P, Shiota M, Shelton KD, Chalkley R, Postic C, Magnuson MA. Phosphoenolpyruvate carboxykinase is necessary for the integration of hepatic energy metabolism. Mol Cell Biol 2000;20(17):6508–17.
[73] Xu J, Xiao G, Trujillo C, Chang V, Blanco L, Joseph SB, et al. Peroxisome proliferator-activated receptor alpha (PPARalpha) influences substrate utilization for hepatic glucose production. J Biol Chem 2002;277(52):50237–44.
[74] Napolitano G, Barone D, Di Meo S, Venditti P. Adrenaline induces mitochondrial biogenesis in rat liver. J Bioenerg Biomembr 2018;50(1):11–9.
[75] Joe Y, Zheng M, Kim HJ, Uddin MJ, Kim SK, Chen Y, et al. Cilostazol attenuates murine hepatic ischemia and reperfusion injury via heme oxygenase-dependent activation of mitochondrial biogenesis. Am J Physiol Gastrointest Liver Physiol 2015;309(1):G21–9.
[76] Puigserver P, Adelmant G, Wu Z, Fan M, Xu J, O'Malley B, et al. Activation of PPARgamma coactivator-1 through transcription factor docking. Science 1999;286(5443):1368–71.
[77] Qian L, Zhu Y, Deng C, Liang Z, Chen J, Chen Y, et al. Peroxisome proliferator-activated receptor gamma coactivator-1 (PGC-1) family in physiological and pathophysiological process and diseases. Signal Transduct Targeted Ther 2024;9(1):50.
[78] Geisler CE, Ghimire S, Hepler C, Miller KE, Bruggink SM, Kentch KP, et al. Hepatocyte membrane potential regulates serum insulin and insulin sensitivity by altering hepatic GABA release. Cell Rep 2021;35(13):109298.
[79] Geisler CE, Ghimire S, Bruggink SM, Miller KE, Weninger SN, Kronenfeld JM, et al. A critical role of hepatic GABA in the metabolic dysfunction and hyperphagia of obesity. Cell Rep 2021;35(13):109301.
[80] van Dyke RW, Gollan JL, Scharschmidt BF. Oxygen consumption by rat liver: effects of taurocholate and sulfobromophthalein transport, glucagon, and cation substitution. Am J Physiol 1983;244(5):G523–31.
[81] Haussinger D. Regulation and functional significance of liver cell volume. Prog Liver Dis 1996;14:29–53.
[82] Russek M. Demonstration of the influence of an hepatic glucosensitive mechanism on food-intake. Physiol Behav 1970;5(10):1207–9.
[83] Russek M, Stevenson JA. Correlation between the effects of several substances on food intake and on the hepatic concentration of reducing sugars. Physiol Behav 1972;8(2):245–9.
[84] Russek M. Current status of the hepatostatic theory of food intake control. Appetite 1981;2(2):137–43.
[85] Stockinger Z, Geary N. 2-Mercaptoacetate stimulates sham feeding in rats. Physiol Behav 1990;47(6):1283–5.
[86] Horn CC, Friedman MI. Methyl palmoxirate increases eating behavior and brain Fos-like immunoreactivity in rats. Brain Res 1998;781(1–2):8–14.
[87] Horn CC, Friedman MI. 2,5-Anhydro-D-mannitol induces fos-like immunoreactivity in hindbrain and forebrain: relationship to eating behavior. Brain Res 1998;779(1–2):17–25.
[88] Horn CC, Kaplan JM, Grill HJ, Friedman MI. Brain fos-like immunoreactivity in chronic decerebrate and neurologically intact rats given 2,5-anhydro-D-mannitol. Brain Res 1998;801(1–2):107–15.
[89] Langhans W, Egli G, Scharrer E. Selective hepatic vagotomy eliminates the hypophagic effect of different metabolites. J Auton Nerv Syst 1985;13(3):255–62.
[90] Friedman MI, Sawchenko PE. Evidence for hepatic involvement in control of ad libitum food intake in rats. Am J Physiol 1984;247(1 Pt 2):R106–13.
[91] Langhans W. The enterocyte as an energy flow sensor in the control of eating. Forum Nutr 2010;63:75–84.
[92] Langhans W, Leitner C, Arnold M. Dietary fat sensing via fatty acid oxidation in enterocytes: possible role in the control of eating. Am J Physiol Regul Integr Comp Physiol 2011;300(3):R554–65.
[93] Berthoud HR, Kressel M, Neuhuber WL. An anterograde tracing study of the vagal innervation of rat liver, portal vein and biliary system. Anat Embryol 1992;186(5):431–42.
[94] Wu C, Kang JE, Peng LJ, Li H, Khan SA, Hillard CJ, et al. Enhancing hepatic glycolysis reduces obesity: differential effects on lipogenesis depend on site of glycolytic modulation. Cell Metab 2005;2(2):131–40.
[95] Visinoni S, Khalid NF, Joannides CN, Shulkes A, Yim M, Whitehead J, et al. The role of liver fructose-1,6-bisphosphatase in regulating appetite and adiposity. Diabetes 2012;61(5):1122–32.
[96] Lopez-Soldado I, Fuentes-Romero R, Duran J, Guinovart JJ. Effects of hepatic glycogen on food intake and glucose homeostasis are mediated by the vagus nerve in mice. Diabetologia 2017;60(6):1076–83.
[97] Uno K, Katagiri H, Yamada T, Ishigaki Y, Ogihara T, Imai J, et al. Neuronal pathway from the liver modulates energy expenditure and systemic insulin sensitivity. Science 2006;312(5780):1656–9.
[98] Bernal-Mizrachi C, Xiaozhong L, Yin L, Knutsen RH, Howard MJ, Arends JJ, et al. An afferent vagal nerve pathway links hepatic PPARalpha activation to glucocorticoid-induced insulin resistance and hypertension. Cell Metab 2007;5(2):91–102.
[99] Uno K, Yamada T, Ishigaki Y, Imai J, Hasegawa Y, Gao J, et al. Hepatic peroxisome proliferator-activated receptor-gamma-fat-specific protein 27 pathway contributes to obesity-related hypertension via afferent vagal signals. Eur Heart J 2012;33(10):1279–89.
[100] Kwon E, Joung HY, Liu SM, Chua Jr SC, Schwartz GJ, Jo YH. Optogenetic stimulation of the liver-projecting melanocortinergic pathway promotes hepatic glucose production. Nat Commun 2020;11(1):6295.
[101] Hwang J, Lee S, Okada J, Liu L, Pessin JE, Chua Jr SC, et al. Liver-innervating vagal sensory neurons are indispensable for the development of hepatic steatosis and anxiety-like behavior in diet-induced obese mice. Nat Commun 2025;16(1):991.

[102] Woodie LN, Melink LC, Midha M, de Araujo AM, Geisler CE, Alberto AJ, et al. Hepatic vagal afferents convey clock-dependent signals to regulate circadian food intake. Science 2024;386(6722):673—7.
[103] Szendroedi J, Chmelik M, Schmid AI, Nowotny P, Brehm A, Krssak M, et al. Abnormal hepatic energy homeostasis in type 2 diabetes. Hepatology 2009;50(4):1079—86.
[104] Nair S, V PC, Arnold C, Diehl AM. Hepatic ATP reserve and efficiency of replenishing: comparison between obese and nonobese normal individuals. Am J Gastroenterol 2003;98(2):466—70.
[105] Chavin KD, Yang S, Lin HZ, Chatham J, Chacko VP, Hoek JB, et al. Obesity induces expression of uncoupling protein-2 in hepatocytes and promotes liver ATP depletion. J Biol Chem 1999;274(9):5692—700.
[106] Schmid AI, Szendroedi J, Chmelik M, Krssak M, Moser E, Roden M. Liver ATP synthesis is lower and relates to insulin sensitivity in patients with type 2 diabetes. Diabetes Care 2011;34(2):448—53.
[107] Fritsch M, Koliaki C, Livingstone R, Phielix E, Bierwagen A, Meisinger M, et al. Time course of postprandial hepatic phosphorus metabolites in lean, obese, and type 2 diabetes patients. Am J Clin Nutr 2015;102(5):1051—8.
[108] Fromenty B, Roden M. Mitochondrial alterations in fatty liver diseases. J Hepatol 2023;78(2):415—29.
[109] Sunny NE, Parks EJ, Browning JD, Burgess SC. Excessive hepatic mitochondrial TCA cycle and gluconeogenesis in humans with nonalcoholic fatty liver disease. Cell Metab 2011;14(6):804—10.
[110] Fletcher JA, Deja S, Satapati S, Fu X, Burgess SC, Browning JD. Impaired ketogenesis and increased acetyl-CoA oxidation promote hyperglycemia in human fatty liver. JCI Insight 2019;5(11).
[111] Satapati S, Sunny NE, Kucejova B, Fu X, He TT, Mendez-Lucas A, et al. Elevated TCA cycle function in the pathology of diet-induced hepatic insulin resistance and fatty liver. J Lipid Res 2012;53(6):1080—92.
[112] Croce MA, Eagon JC, LaRiviere LL, Korenblat KM, Klein S, Finck BN. Hepatic lipin 1beta expression is diminished in insulin-resistant obese subjects and is reactivated by marked weight loss. Diabetes 2007;56(9):2395—9.
[113] Cortez-Pinto H, Chatham J, Chacko VP, Arnold C, Rashid A, Diehl AM. Alterations in liver ATP homeostasis in human nonalcoholic steatohepatitis: a pilot study. JAMA 1999;282(17):1659—64.
[114] Bawden SJ, Stephenson MC, Ciampi E, Hunter K, Marciani L, Macdonald IA, et al. Investigating the effects of an oral fructose challenge on hepatic ATP reserves in healthy volunteers: a (31)P MRS study. Clin Nutr 2016;35(3):645—9.
[115] Abdelmalek MF, Lazo M, Horska A, Bonekamp S, Lipkin EW, Balasubramanyam A, et al. Higher dietary fructose is associated with impaired hepatic adenosine triphosphate homeostasis in obese individuals with type 2 diabetes. Hepatology 2012;56(3):952—60.
[116] Koliaki C, Szendroedi J, Kaul K, Jelenik T, Nowotny P, Jankowiak F, et al. Adaptation of hepatic mitochondrial function in humans with non-alcoholic fatty liver is lost in steatohepatitis. Cell Metab 2015;21(5):739—46.
[117] Moore MP, Cunningham RP, Meers GM, Johnson SA, Wheeler AA, Ganga RR, et al. Compromised hepatic mitochondrial fatty acid oxidation and reduced markers of mitochondrial turnover in human NAFLD. Hepatology 2022;76(5):1452—65.
[118] Morris EM, McCoin CS, Allen JA, Gastecki ML, Koch LG, Britton SL, et al. Aerobic capacity mediates susceptibility for the transition from steatosis to steatohepatitis. J Physiol 2017;595(14):4909—26.
[119] Morris EM, Meers GM, Koch LG, Britton SL, Fletcher JA, Fu X, et al. Aerobic capacity and hepatic mitochondrial lipid oxidation alters susceptibility for chronic high-fat diet-induced hepatic steatosis. Am J Physiol Endocrinol Metab 2016;311(4):E749—60.
[120] Poussin C, Ibberson M, Hall D, Ding J, Soto J, Abel ED, et al. Oxidative phosphorylation flexibility in the liver of mice resistant to high-fat diet-induced hepatic steatosis. Diabetes 2011;60(9):2216—24.
[121] Eccleston HB, Andringa KK, Betancourt AM, King AL, Mantena SK, Swain TM, et al. Chronic exposure to a high-fat diet induces hepatic steatosis, impairs nitric oxide bioavailability, and modifies the mitochondrial proteome in mice. Antioxidants Redox Signal 2011;15(2):447—59.
[122] Echeverria F, Valenzuela R, Bustamante A, Alvarez D, Ortiz M, Espinosa A, et al. High-fat diet induces mouse liver steatosis with a concomitant decline in energy metabolism: attenuation by eicosapentaenoic acid (EPA) or hydroxytyrosol (HT) supplementation and the additive effects upon EPA and HT co-administration. Food Funct 2019;10(9):6170—83.
[123] Ortiz M, Soto-Alarcon SA, Orellana P, Espinosa A, Campos C, Lopez-Arana S, et al. Suppression of high-fat diet-induced obesity-associated liver mitochondrial dysfunction by docosahexaenoic acid and hydroxytyrosol co-administration. Dig Liver Dis 2020;52(8):895—904.
[124] Lee K, Haddad A, Osme A, Kim C, Borzou A, Ilchenko S, et al. Hepatic mitochondrial defects in a nonalcoholic fatty liver disease mouse model are associated with increased degradation of oxidative phosphorylation subunits. Mol Cell Proteomics 2018;17(12):2371—86.
[125] Garcia-Ruiz I, Solis-Munoz P, Fernandez-Moreira D, Grau M, Colina F, Munoz-Yague T, et al. High-fat diet decreases activity of the oxidative phosphorylation complexes and causes nonalcoholic steatohepatitis in mice. Dis Model Mech 2014;7(11):1287—96.
[126] Aharoni-Simon M, Hann-Obercyger M, Pen S, Madar Z, Tirosh O. Fatty liver is associated with impaired activity of PPARgamma-coactivator 1alpha (PGC1alpha) and mitochondrial biogenesis in mice. Lab Invest 2011;91(7):1018—28.
[127] Fouret G, Gaillet S, Lecomte J, Bonafos B, Djohan F, Barea B, et al. 20-Week follow-up of hepatic steatosis installation and liver mitochondrial structure and activity and their interrelation in rats fed a high-fat-high-fructose diet. Br J Nutr 2018;119(4):368—80.
[128] Perez-Carreras M, Del Hoyo P, Martin MA, Rubio JC, Martin A, Castellano G, et al. Defective hepatic mitochondrial respiratory chain in patients with nonalcoholic steatohepatitis. Hepatology 2003;38(4):999—1007.
[129] Mantena SK, Vaughn DP, Andringa KK, Eccleston HB, King AL, Abrams GA, et al. High fat diet induces dysregulation of hepatic oxygen gradients and mitochondrial function in vivo. Biochem J 2009;417(1):183—93.
[130] Wang X, Wang J, Ying C, Xing Y, Su X, Men K. Fenofibrate alleviates NAFLD by enhancing the PPARalpha/PGC-1alpha signaling pathway coupling mitochondrial function. BMC Pharmacol Toxicol 2024;25(1):7.
[131] Abrahams Y, Willmer T, Patel O, Samodien E, Muller CJF, Windvogel S, et al. A high fat, high sugar diet induces hepatic peroxisome proliferator-activated receptor gamma coactivator 1-alpha promoter hypermethylation in male Wistar rats. Biochem Biophys Res Commun 2023;680:25—33.
[132] Wang SW, Sheng H, Bai YF, Weng YY, Fan XY, Lou LJ, et al. Neohesperidin enhances PGC-1alpha-mediated mitochondrial biogenesis and alleviates hepatic steatosis in high fat diet fed mice. Nutr Diabetes 2020;10(1):27.
[133] Bhaskaran S, Pharaoh G, Ranjit R, Murphy A, Matsuzaki S, Nair BC, et al. Loss of mitochondrial protease ClpP protects mice from diet-induced obesity and insulin resistance. EMBO Rep 2018;19(3).
[134] Barroso WA, Victorino VJ, Jeremias IC, Petroni RC, Ariga SKK, Salles TA, et al. High-fat diet inhibits PGC-1alpha suppressive effect on NFkappaB signaling in hepatocytes. Eur J Nutr 2018;57(5):1891—900.
[135] Thyfault JP, Morris EM. Intrinsic (genetic) aerobic fitness impacts susceptibility for metabolic disease. Exerc Sport Sci Rev 2017;45(1):7—15.
[136] Westerbacka J, Kolak M, Kiviluoto T, Arkkila P, Siren J, Hamsten A, et al. Genes involved in fatty acid partitioning and binding, lipolysis, monocyte/macrophage recruitment, and inflammation are overexpressed in the human fatty liver of insulin-resistant subjects. Diabetes 2007;56(11):2759—65.
[137] Wan X, Zhu X, Wang H, Feng Y, Zhou W, Liu P, et al. PGC1alpha protects against hepatic steatosis and insulin resistance via enhancing IL10-mediated anti-inflammatory response. FASEB J 2020;34(8):10751—61.

[138] Orellana-Gavalda JM, Herrero L, Malandrino MI, Paneda A, Sol Rodriguez-Pena M, Petry H, et al. Molecular therapy for obesity and diabetes based on a long-term increase in hepatic fatty-acid oxidation. Hepatology 2011;53(3):821–32.
[139] Cork SC. The role of the vagus nerve in appetite control: implications for the pathogenesis of obesity. J Neuroendocrinol 2018;30(11):e12643.
[140] de Lartigue G. Putative roles of neuropeptides in vagal afferent signaling. Physiol Behav 2014;136:155–69.
[141] de Lartigue G. Role of the vagus nerve in the development and treatment of diet-induced obesity. J Physiol 2016;594(20):5791–815.
[142] Page AJ, Kentish SJ. Plasticity of gastrointestinal vagal afferent satiety signals. Neuro Gastroenterol Motil 2017;29(5).
[143] Stanimirovic J, Obradovic M, Panic A, Petrovic V, Alavantic D, Melih I, et al. Regulation of hepatic Na(+)/K(+)-ATPase in obese female and male rats: involvement of ERK1/2, AMPK, and Rho/ROCK. Mol Cell Biochem 2018;440(1–2):77–88.
[144] Langhans W, Scharrer E. Evidence for a role of the sodium pump of hepatocytes in the control of food intake. J Auton Nerv Syst 1987;20(3):199–205.
[145] Boutellier S, Lutz TA, Volkert M, Scharrer E. 2-Mercaptoacetate, an inhibitor of fatty acid oxidation, decreases the membrane potential in rat liver in vivo. Am J Physiol 1999;277(1):R301–5.
[146] Haylett DG, Jenkinson DH. Effects of noradrenaline on potassium reflux, membrane potential and electrolyte levels in tissue slices prepared from guinea-pig liver. J Physiol 1972;225(3):721–50.
[147] Claret B, Claret M, Mazet JL. Ionic transport and membrane potential of rat liver cells in normal and low-chloride solutions. J Physiol 1973;230(1):87–101.
[148] Cermak R, Scharrer E. Effect of 2,5-anhydro-D-mannitol on membrane potential in rat hepatocyte couplets and hepatocyte monolayer cultures. Biochim Biophys Acta 1999;1421(1):116–24.
[149] Wondergem R, Harder DR. Transmembrane potential and amino acid transport in rat hepatocytes in primary monolayer culture. J Cell Physiol 1980;104(1):53–60.
[150] Fitz JG, Scharschmidt BF. Regulation of transmembrane electrical potential gradient in rat hepatocytes in situ. Am J Physiol 1987;252(1 Pt 1):G56–64.
[151] Minuk GY, Vergalla J, Ferenci P, Jones EA. Identification of an acceptor system for gamma-aminobutyric acid on isolated rat hepatocytes. Hepatology 1984;4(2):180–5.
[152] van der Laan JW, de Boer T, Bruinvels J. Di-n-propylacetate and GABA degradation. Preferential inhibition of succinic semialdehyde dehydrogenase and indirect inhibition of GABA-transaminase. J Neurochem 1979;32(6):1769–80.
[153] Clausen MV, Hilbers F, Poulsen H. The structure and function of the Na,K-ATPase isoforms in health and disease. Front Physiol 2017;8:371.
[154] Yap JQ, Seflova J, Sweazey R, Artigas P, Robia SL. FXYD proteins and sodium pump regulatory mechanisms. J Gen Physiol 2021;153(4).
[155] Jensen-Cody SO, Potthoff MJ. Hepatokines and metabolism: deciphering communication from the liver. Mol Metabol 2021;44:101138.
[156] Fletcher JA, Linden MA, Sheldon RD, Meers GM, Morris EM, Butterfield A, et al. Fibroblast growth factor 21 increases hepatic oxidative capacity but not physical activity or energy expenditure in hepatic peroxisome proliferator-activated receptor gamma coactivator-1alpha-deficient mice. Exp Physiol 2018;103(3):408–18.
[157] Nahon JL, Tratner I, Poliard A, Presse F, Poiret M, Gal A, et al. Albumin and alpha-fetoprotein gene expression in various nonhepatic rat tissues. J Biol Chem 1988;263(23):11436–42.
[158] Martin SL, Epperson LE, Rose JC, Kurtz CC, Ane C, Carey HV. Proteomic analysis of the winter-protected phenotype of hibernating ground squirrel intestine. Am J Physiol Regul Integr Comp Physiol 2008;295(1):R316–28.
[159] Meehan RR, Barlow DP, Hill RE, Hogan BL, Hastie ND. Pattern of serum protein gene expression in mouse visceral yolk sac and foetal liver. EMBO J 1984;3(8):1881–5.
[160] Borengasser SJ, Faske J, Kang P, Blackburn ML, Badger TM, Shankar K. In utero exposure to prepregnancy maternal obesity and postweaning high-fat diet impair regulators of mitochondrial dynamics in rat placenta and offspring. Physiol Genom 2014;46(23):841–50.
[161] Burgueno AL, Cabrerizo R, Gonzales Mansilla N, Sookoian S, Pirola CJ. Maternal high-fat intake during pregnancy programs metabolic-syndrome-related phenotypes through liver mitochondrial DNA copy number and transcriptional activity of liver PPARGC1A. J Nutr Biochem 2013;24(1):6–13.
[162] Desai M, Ferrini MG, Han G, Narwani K, Ross MG. Maternal high fat diet programs Male mice offspring hyperphagia and obesity: mechanism of increased appetite neurons via altered neurogenic factors and nutrient sensor AMPK. Nutrients 2020;12(11).

